NATIONAL ADVISORY COMMITTEE
FOR AERONAUTICS

TECHNICAL NOTE 2873

THE EFFECT OF LONGITUDINAL STIFFENERS LOCATED ON ONE SIDE

OF A PLATE ON THE COMPRESSIVE BUCKLING STRESS

OF THE PLATE-STIFFENER COMBINATION

By Paul Seide

Langley Aeronautical Laboratory
Langley Field, Va.

NACA

Washington

January 1953

NATIONAL ADVISORY COMMITTEE FOR AERONAUTIC

TECHNICAL NOTE 2873

THE EFFECT OF LONGITUDINAL STIFFENERS LOCATED ON ONE SIDE

OF A PLATE ON THE COMPRESSIVE BUCKLING STRESS

OF THE PLATE-STIFFENER COMBINATION

By Paul Seide

SUMMARY

The problem of buckling under uniform compression of flat, simply supported, rectangular plates with equally spaced longitudinal stiffeners on one side of the plate is investigated. For the case of a plate with one, two, or infinitely many stiffeners, the analysis yields expressions for the effective moment of inertia of the stiffeners that can be used in conjunction with the buckling charts previously presented in NACA TN 1825.

INTRODUCTION

The buckling of stiffened plates is a subject which has received much attention in the literature on aircraft structures. With few exceptions, the solutions presented are idealized and are valid only for stiffened plates for which the center of gravity of each stiffener cross section lies in the middle surface of the plate or for which the stiffeners are hypothetically connected to the plate in such a manner that sliding of the stiffener along the plate surface is permitted. Although these solutions clearly establish the relationship between the buckling stress of the plate stiffener combination and the flexural stiffness of the stiffener, they do not determine the effective flexural stiffness provided by stiffeners in the usual aircraft application, that is, when they are riveted to one side of the plate.

Timoshenko suggested (ref. 1) that the stiffness of a one-sided stiffener might be taken into account by replacing the moment of inertia of the stiffener about its center of gravity by an effective moment of inertia and using this value in the solutions valid for stiffeners with their centers of gravity located in the plate middle surface. In several illustrative examples he took this effective moment of inertia as the moment of inertia of the stiffener cross section about the plane of contact with the plate. That this method of correction is arbitrary and not generally applicable to all plate stiffener proportions, however, can

be readily seen. If the stiffeners are very large compared to the plate, the attached plate can have very little effect on the bending of each stiffener about an axis passing through the center of gravity of the stiffener cross section. On the other hand, stiffeners that are very small compared to the plate would appear to be forced to bend about the plate middle surface. The effective moment of inertia of a given stiffener can therefore vary between the moment of inertia taken about the center of gravity of the stiffener cross section and the moment of inertia taken about the plate middle surface depending upon the proportions of the attached plate. For Z-stiffeners of the proportions encountered in aircraft construction, the ratio of the moments of inertia based on these two limiting positions for the assumed neutral axis of bending is greater than 2.5 to 1. Because the effective moment of inertia chosen to represent a given stiffener strongly influences the calculated buckling stress of the plate stiffener combination, it is therefore desirable that any arbitrariness in its calculation be eliminated.

Investigations of plates with stiffeners on one side have been made and verify the dependence of the effective moment of inertia of the stiffener on the relative dimensions of the plate and stiffener. These solutions, however, are generally limited to special cases. The bending of an infinitely wide plate with a longitudinal stiffener on one side is investigated in references 2 to 4. In reference 2, Timoshenko and Goodier neglect the flexural stiffness of the plate and consider loads applied only to the stiffener; an extension is made in reference 3 by Smith, Heebink, and Norris to include the plate flexural stiffness; both plate flexural stiffness and loads applied to the plate are considered by Odqvist in reference 4. Shear buckling of a finite-width plate with a centrally located longitudinal stiffener on one side is investigated by Chwalla and Novak in reference 5. Good accuracy would be expected in their analysis only when the plate is relatively wide. Cox and Riddell (ref. 6) give an expression based on an effective-width concept for the effective stiffener stiffness for compressive buckling of a finite width plate with a centrally located longitudinal stiffener on one side. The stability of plates with closely spaced longitudinal and transverse stiffeners is investigated approximately by Freyer in reference 7. A very accurate set of differential equations for the same problem is developed by Pfluger in reference 8. These differential equations contain terms which reflect the consideration of changes of geometry of the plate beyond those considered in the elementary theory of bending and buckling of flat plates. The contribution of these terms is shown to be insignificant, however, in the practical range of stiffened-plate construction.

The references cited indicate that some studies have been made of the buckling behavior of plates with one stiffener or with many closely spaced stiffeners. No material appeared to be available for the cases that fall between these extremes. In the present paper, a unified analysis is made of the buckling behavior under uniform compression of a flat, rectangular, simply supported plate with one, two, three, or infinitely

many longitudinal stiffeners located on one side of the plate. The essential feature of the results of this analysis is that the effective moment of inertia of one-sided stiffeners on plates of arbitrary dimensions can be written in terms of a simple correction to the moment of inertia of the stiffeners about their own centers of gravity. This effective moment of inertia can then be used in conjunction with the buckling charts of the type previously presented in reference 9. The analysis leading to this result is given in the appendixes.

The material presented herein was submitted to the University of Virginia in partial fulfillment of the requirements for a masters degree.

SYMBOLS

A_S	stiffener area
a	plate length
a_n	Fourier coefficients in bending deflection function
b	plate width, Nd
D	plate flexural stiffness, $\dfrac{Et^3}{12(1 - \mu^2)}$
d	bay width
E	Young's modulus for plate and stiffeners
F_i	shear force per unit length applied at ith contact line for plates with one, two, or three stiffeners
F_∞	shear force per unit length applied at any contact line for infinitely many stiffeners
F_{im}	coefficients of shear forces for plates with one, two, or three stiffeners
$F_m{}'$	coefficients of shear forces for plates with infinitely many stiffeners
j,s	integers
i	integer denoting contact line or bay
k	number denoting location of contact line with respect to plate center line

I_S moment of inertia of stiffener cross section, taken about axis parallel to plane of plate and passing through center of gravity of stiffener cross section.

I_{eff} effective moment of inertia of stiffener

m integer denoting number of buckle half-waves in longitudinal direction

N number of bays

$N_{x_i}, N_{y_i}, N_{xy_i}$ additional forces per unit width in plane of plate middle surface in ith bay

n, r integers denoting mode of buckling

P_i additional load in ith stiffener

p, q integers denoting number of buckle half-waves in transverse direction

t plate thickness

U total potential energy of stiffened plate

u middle-surface displacement

u_i, v_i additional displacements in plane of plate middle surface in x- and y-directions in ith bay, respectively

u_{S_i} additional displacements in x-direction at center of gravity of cross section of ith stiffener

V strain energy

W potential energy

w bending deflection, normal to plane of plate

x, y distances along coordinate axes (see fig. 1)

Z_{Nq} modal coefficient appearing in expression for effective moment of inertia of stiffeners

$\bar{z}_S$ distance normal to plane of plate between plate middle surface and center of gravity of stiffener cross section

$\epsilon_{x_i}, \epsilon_{y_i}, \gamma_{xy_i}$ additional direct and shear strains in plane of plate middle surface in ith bay

ϵ_{S_i} additional direct strains at center of gravity of cross
                                     section of ith stiffener

$\eta_1, \eta_2, \eta_3,$ modal coefficients appearing in criterion for buckling
                                     symmetrical about longitudinal center line of plate
η_4, η_5, η_6 with three stiffeners

μ Poisson's ratio for plate material

$$\theta_1 = \pi \sqrt{\frac{m}{a/d}\left(\sqrt{\frac{d^2\bar{\sigma}_x t}{\pi^2 D}} - \frac{m}{a/d}\right)}$$

$$\theta_2 = \pi \sqrt{\frac{m}{a/d}\left(\sqrt{\frac{d^2\bar{\sigma}_x t}{\pi^2 D}} + \frac{m}{a/d}\right)}$$

$\bar{\sigma}_x$ uniform longitudinal compressive stress

$$\nabla^2 = \frac{\partial^2}{\partial x^2} + \frac{\partial^2}{\partial y^2}$$

$$\nabla^4 = \frac{\partial^4}{\partial x^4} + 2\frac{\partial^4}{\partial x^2 \partial y^2} + \frac{\partial^4}{\partial y^4}$$

$\dfrac{d^2\bar{\sigma}_x t}{\pi^2 D}$ buckling-stress parameter

$\dfrac{a/d}{m}$ buckle aspect ratio

a/d aspect ratio of each bay

$\dfrac{EI_S}{dD}$ flexural-stiffness ratio (called γ in ref. 9)

$\dfrac{EI_{eff}}{dD}$ effective-flexural-stiffness ratio

$\dfrac{A_S}{dt}$ area ratio

Subscripts:

N   number of bays

P   plate

S   stiffeners

RESULTS AND DISCUSSION

Statement of the Problem

The problem that is investigated in the present paper is the determination of the buckling stress of a flat, simply supported, rectangular plate with one, two, three, or an infinite number of longitudinal stiffeners on one side. The stiffeners are equally spaced, are each of the same cross section, and have a Young's modulus equal to that of the plate. (See fig. 1.) The plate is loaded by uniform compressive forces per unit width $\bar{\sigma}_x t$ on its transverse edges and the end load on each stiffener is a compressive force $\bar{\sigma}_x A_S$.

Assumptions and Limitations of Analysis

The assumptions and limitations of the analysis are as follows:

(1) Each stiffener is assumed to be continuously and rigidly connected to the plate along a straight line (the contact line) in the plate middle surface. This condition may be visualized by supposing the stiffener to be extended to the contact line by a rod of infinitesimal area. (See fig. 2.) The effects of rivet spacing and of rivet flexibility are thus excluded from the analysis.

(2) Each stiffener is assumed to have zero flexural stiffness for bending parallel to the plane of the plate and zero torsional stiffness.

(3) Small-deflection theory for bending of elastic plates and elementary beam theory for bending of the stiffeners are used. The analysis is thus limited to a general instability of the plate-stiffener combination and excludes such effects as local buckling of stiffeners, cross-sectional distortions, and shear deformations of the stiffeners, all of which decrease the effective moment of inertia of the stiffener.

(4) An artifical boundary condition is introduced into the analysis; that is, points in the transverse edges of the plate are taken to be free to move transversely before buckling occurs but are completely restrained from further movement after buckling. Any other boundary conditions would needlessly complicate the analysis. The longitudinal edges of the plate are taken to be free from middle-surface forces both before and after buckling.

Summary of Analysis

The stability criterions for compressive buckling of longitudinally stiffened plates with deflection of the stiffeners, derived in appendix A, with the exception of the criterion for buckling symmetrical about the longitudinal center line of a plate with three stiffeners, can be expressed as follows:

$$\frac{EI_S}{dD} + \frac{1}{1 + Z_{Nq}\frac{A_S}{dt}}\frac{EA_S\bar{z}_S^2}{dD} = \frac{\frac{4}{\pi^2}\left(\frac{a/d}{m}\right)^3\sqrt{\frac{d^2\bar{\sigma}_x t}{\pi^2 D}}}{\dfrac{\sin\theta_1}{\theta_1}}{\cos\frac{\pi q}{N} - \cos\theta_1} - \dfrac{\frac{\sinh\theta_2}{\theta_2}}{\cos\frac{\pi q}{N} - \cosh\theta_2} + \frac{d^2\bar{\sigma}_x t}{\pi^2 D}\left(\frac{a/d}{m}\right)^2\frac{A_S}{dt}$$

$$(1)$$

where

$$\left.\begin{aligned}\theta_1 &= \pi\sqrt{\frac{m}{a/d}\left(\sqrt{\frac{d^2\bar{\sigma}_x t}{\pi^2 D}} - \frac{m}{a/d}\right)}\\[2ex]\theta_2 &= \pi\sqrt{\frac{m}{a/d}\left(\sqrt{\frac{d^2\bar{\sigma}_x t}{\pi^2 D}} + \frac{m}{a/d}\right)}\end{aligned}\right\}\quad(2)$$

$$(m = 1,\ 2,\ 3,\ \ldots\ \infty)$$

and Z_{Nq} is a modal coefficient. This modal coefficient is a function of the buckle aspect ratio $\frac{a/d}{m}$, the number of bays N, and the mode of buckling indicated by q as in the following table:

Number of bays, N	Number of stiffeners, N − 1	q	Mode of buckling about longitudinal center line of plate
2	1	1	Symmetrical
3	2	1	Symmetrical
		2	Antisymmetrical
4	3	2	Antisymmetrical
∞	∞	$\frac{q}{N} = 0$	Symmetrical

The variation of Z_{Nq} with the buckle aspect ratio $\dfrac{a/d}{m}$ is shown in table I and in figure 3. Poisson's ratio μ was taken as 1/3 in the calculation of these values.

The criterion for buckling symmetrical about the longitudinal center line of a plate with three stiffeners is given by

$$\left[\frac{EI_S}{dD} + \frac{1 + \eta_1 \frac{A_S}{dt}}{\left(1 + \eta_2 \frac{A_S}{dt}\right)\left(1 + \eta_3 \frac{A_S}{dt}\right) - \left(\eta_4 \frac{A_S}{dt}\right)^2} \frac{EA_S \bar{z}_S^2}{dD} - \frac{d^2 \bar{\sigma}_x t}{\pi^2 D}\left(\frac{a/d}{m}\right)^2 \frac{A_S}{dt} - \right.$$

$$\left. \frac{\frac{4}{\pi^2}\left(\frac{a/d}{m}\right)^3 \sqrt{\frac{d^2 \bar{\sigma}_x t}{\pi^2 D}}}{\dfrac{\frac{\sin \theta_1}{\theta_1}}{\frac{\sqrt{2}}{2} - \cos \theta_1} - \dfrac{\frac{\sinh \theta_2}{\theta_2}}{\frac{\sqrt{2}}{2} - \cosh \theta_2}} \right]\left[\frac{EI_S}{dD} + \frac{1 + \eta_5 \frac{A_S}{dt}}{\left(1 + \eta_2 \frac{A_S}{dt}\right)\left(1 + \eta_3 \frac{A_S}{dt}\right) - \left(\eta_4 \frac{A_S}{dt}\right)^2} \frac{EA_S \bar{z}_S^2}{dD} - \right.$$

$$\left. \frac{d^2 \bar{\sigma}_x t}{\pi^2 D}\left(\frac{a/d}{m}\right)^2 \frac{A_S}{dt} - \frac{\frac{4}{\pi^2}\left(\frac{a/d}{m}\right)^3 \sqrt{\frac{d^2 \bar{\sigma}_x t}{\pi^2 D}}}{\dfrac{\frac{\sinh \theta_2}{\theta_2}}{\frac{\sqrt{2}}{2} + \cosh \theta_2} - \dfrac{\frac{\sin \theta_1}{\theta_1}}{\frac{\sqrt{2}}{2} + \cos \theta_1}} \right] -$$

$$\left[\frac{\eta_6 \frac{A_S}{dt}}{\left(1 + \eta_2 \frac{A_S}{dt}\right)\left(1 + \eta_3 \frac{A_S}{dt}\right) - \left(\eta_4 \frac{A_S}{dt}\right)^2} \frac{EA_S \bar{z}_S^2}{dD} \right]^2 = 0 \qquad (3)$$

$$(m = 1, 2, \ldots \infty)$$

where η_1 to η_6 are modal coefficients and are functions of $\dfrac{a/d}{m}$.
The variation of η_1 to η_6 with $\dfrac{a/d}{m}$ is given in table II and is shown graphically in figure 4.

When buckling symmetrical about the longitudinal center line of a plate with one, two, or infinitely many longitudinal stiffeners on one side is investigated, the buckling charts of reference 9 may be used. In place of the flexural-stiffness ratio $\dfrac{EI}{dD}$, these charts are entered with values of the effective-flexural-stiffness ratio

$$\frac{EI_{eff}}{dD} = \frac{EI_S}{dD} + \frac{1}{1 + Z_{Nq}\dfrac{A_S}{dt}}\frac{EA_S\bar{z}_S^2}{dD} \tag{4}$$

where EI_{eff}/dD is calculated with the proper value of the modal coefficient Z_{Nq} obtained from table I or from figure 3 of the present paper. Thus, if the buckling-stress parameter for a certain plate-stiffener combination is desired, the chart of reference 9 for the appropriate area ratio and number of stiffeners is entered with EI_{eff}/dD and the given value of the plate-bay aspect ratio to obtain the buckling-stress parameter. In this procedure, the value of m used in reading Z_{Nq} from figure 3 of the present paper must correspond to the value of m in the region of the charts of reference 9 from which the buckling-stress parameter is read. In the charts of reference 9, the value of m in the region to the left of the first dashed-line curve is 1 and the value of m in the region to the right of that curve is 2; m would increase in value by 1 in the region to the right of each succeeding dashed-line curve.

When buckling symmetrical about the longitudinal center line of a plate with three stiffeners on one side is investigated, equation (3) must be solved by trial and error for the value of the buckling-stress parameter corresponding to a given value of m. Different values of m are tried until a minimum value of the buckling-stress parameter is obtained.

Investigation of the antisymmetrical modes of buckling for plates with two or three stiffeners involves a trial-and-error solution of equation (1) for the buckling-stress parameter for given physical dimensions of plate and stiffeners.

For each case the criterion for buckling with nodes at each stiffener

$$\frac{d^2 \sigma_x t}{\pi^2 d} = \left(\frac{m}{a/d} + \frac{a/d}{m} \right)^2 \tag{5}$$

should be checked since this criterion defines the highest buckling-stress parameter obtainable in conjunction with an assumption of zero torsional stiffness for the stiffeners.

CONCLUDING REMARKS

The buckling under uniform compression of flat, simply supported, rectangular plates with equally spaced longitudinal stiffeners each of the same cross section and a Young's modulus equal to that of the plate is investigated. The effect of one-sided placement of stiffeners on the plate is incorporated in a simple expression for the effective moment of inertia of the stiffeners. For a plate with one, two, or infinitely many stiffeners, the effective moment of inertia can be used in conjunction with buckling charts of the type previously presented in NACA TN 1825. For a plate with three stiffeners, a new stability criterion is derived.

Langley Aeronautical Laboratory,
        National Advisory Committee for Aeronautics,
                Langley Field, Va., June 16, 1952.

APPENDIX A

STABILITY ANALYSIS OF PLATES WITH ONE-SIDED STIFFENERS

Determination of Stress Distribution in the Buckled Plate

Consider the bending of a plate with stiffeners attached so that sliding of the plate and stiffeners is permitted. Middle-surface displacements u in the plate along each contact line exist and in each stiffener there exist contact-line displacements $u_S + \bar{z}_S \frac{\partial w}{\partial x}$, where u_S is the displacement at the center of gravity of the stiffener cross section and $\bar{z}_S \frac{\partial w}{\partial x}$ represents the displacement due to bending, the cross sections of the stiffener being assumed to remain plane and perpendicular to the deformed axis of the stiffener. In general, u and $u_S + \bar{z}_S \frac{\partial w}{\partial x}$ are unequal and there would exist relative displacements of corresponding points of the plate and stiffeners. $\Big($In the present problem, for example, if the stiffeners were permitted to slide along the sheet, u and u_S would be equal but relative displacements due to bending, of magnitude $\bar{z}_S \frac{\partial w}{\partial x}$, would exist.$\Big)$ Since in an actual plate these relative displacements are not permitted, a system of shear forces, which produce additional deformations to cancel out the relative displacements, are induced in the structure. The system of shear forces consists of forces applied to the plate middle surface at each contact line and equal but opposite forces applied to the corresponding stiffener at each contact line. The effect of these forces on the buckling stress of a stiffened plate loaded in edge compression is investigated in the present paper.

Prior to buckling, the stiffened plate considered herein is uniformly compressed, the longitudinal direct stress in both the plate and stiffener being equal to $-\bar{\sigma}_x$; all other stresses in the plate are equal to zero. When the stiffened plate buckles, however, self-equilibrating shear forces are induced at each contact line within the structure, as demonstrated previously, and the stress distribution within the plate changes although the applied edge stresses remain constant. The additional stresses in the structure must be investigated before the buckling stress of the stiffened plate can be determined.

Within each bay of the plate the additional middle-surface forces are continuous and in equilibrium, that is, for the ith bay

$$
\left.
\begin{aligned}
\frac{\partial N_{x_i}}{\partial x} + \frac{\partial N_{xy_i}}{\partial y} &= 0 \\[2em]
\frac{\partial N_{y_i}}{\partial y} + \frac{\partial N_{xy_i}}{\partial x} &= 0
\end{aligned}
\right\} \tag{A1}
$$

and are related to the middle-surface strains in the ith bay by

$$
\left.
\begin{aligned}
\epsilon_{x_i} &= \frac{1}{Et}\left(N_{x_i} - \mu N_{y_i}\right) \\[1.5em]
\epsilon_{y_i} &= \frac{1}{Et}\left(N_{y_i} - \mu N_{x_i}\right) \\[1.5em]
\gamma_{xy_i} &= \frac{2(1 + \mu)}{Et}\, N_{xy_i}
\end{aligned}
\right\} \tag{A2}
$$

Strains are related to middle-surface displacements by the expressions

$$
\left.
\begin{aligned}
\epsilon_{x_i} &= \frac{\partial u_i}{\partial x} \\[1.5em]
\epsilon_{y_i} &= \frac{\partial v_i}{\partial y} \\[1.5em]
\gamma_{xy_i} &= \frac{\partial u_i}{\partial y} + \frac{\partial v_i}{\partial x}
\end{aligned}
\right\} \tag{A3}
$$

From the boundary conditions given in the section entitled "Assumptions and Limitations of Analysis," normal and tangential middle-surface forces must vanish along the longitudinal edges of the plate and

normal middle-surface forces and tangential displacements must vanish along the transverse edges of the plate; that is, at $y = \frac{Nd}{2}$,

$$N_{y_N} = N_{xy_N} = 0 \tag{A4a}$$

at $y = -\frac{Nd}{2}$,

$$N_{y_1} = N_{xy_1} = 0 \tag{A4b}$$

and, at $x = 0$ and $x = a$,

$$N_{x_i} = v_i = 0 \qquad (i = 1, 2, \ldots N) \tag{A4c}$$

In addition, the following conditions must be satisfied along each contact line:

$$\left.\begin{aligned}
N_{xy_i} - N_{xy_{i+1}} &= F_i \\[2mm]
N_{y_i} &= N_{y_{i+1}} \\[2mm]
u_i &= u_{i+1} \\[2mm]
v_i &= v_{i+1}
\end{aligned}\right\} \quad (i = 1, 2, \ldots (N-1)) \tag{A5}$$

where F_i is the shear force per unit length induced at the ith contact line after buckling. These conditions state that at each contact line the difference of the shears in adjacent bays is equal to the applied shear load, that middle-surface forces normal to the longitudinal edges of adjacent bays are continuous, and that middle-surface displacements are continuous.

The additional forces and displacements along the centroidal axis of the stiffeners due to the shear forces induced after buckling are

found from the equations of equilibrium of shear force and internal
load to be

$$\frac{dP_i}{dx} = F_i \qquad (i = 1, 2, \ldots (N - 1)) \qquad \text{(A6)}$$

and the load-strain relationships are found to be

$$\epsilon_{S_i} = \frac{P_i}{A_S E} \qquad (i = 1, 2, \ldots (N - 1)) \qquad \text{(A7)}$$

where

$$\epsilon_{S_i} = \frac{du_{S_i}}{dx} \qquad \text{(A8)}$$

with the conditions that each load P_i must vanish at the ends of the
corresponding stiffener.

The appropriate expressions for the shear force at each contact
line are now assumed to be

$$F_i = F_{im} \cos \frac{m\pi x}{a} \qquad (i = 1, 2, \ldots (N - 1)) \qquad \text{(A9)}$$

where m is an integer. (It will be seen subsequently that this result
is consistent with the assumption of sinusoidal buckling with m half-
waves in the longitudinal direction and that this type of buckling
actually occurs.) The forces and displacements in the plate and in the
stiffeners due to a single shear force of the form of equation (A9),
located anywhere in the plate, are derived in appendix B. The middle-
surface forces and displacements at any point in the plate due to all
the shear forces are obtained by superposing the individual forces and
displacements at the point due to each of the shear forces.

Thus far in the discussion the shear forces induced by contact-
line restraint have been considered arbitrary. They can be related,
however, to the bending deflections of the plate middle surface by
conditions of continuity of plate and stiffener at each contact line.
When buckling occurs, the addition displacements at each contact line
in the plate due to the induced shear forces are $\left(u_1\right)_{y=\left(i - \frac{N}{2}\right)d}$ and the

contact-line displacements in the stiffeners are $u_{s_i} + \bar{z}_s\left(\frac{\partial w}{\partial x}\right)_{y=\left(i-\frac{N}{2}\right)d}$

In order for points in the plate and stiffeners to remain together, these two displacements must be equal at every point in the contact line. Then

$$u_{s_i} + \bar{z}_s\left(\frac{\partial w}{\partial x}\right)_{y=\left(i-\frac{N}{2}\right)d} = \left(u_i\right)_{y=\left(i-\frac{N}{2}\right)d} \tag{A10}$$

$$(i = 1, 2, \ldots (N-1))$$

An appropriate expression for the bending deflections of the stiffened plate is

$$w = \sin\frac{m\pi x}{a}\sum_{n=1}^{\infty} a_n \sin\frac{n\pi}{2}\left(\frac{2y}{Nd} + 1\right) \tag{A11}$$

When equation (A11) and the displacements in the plate and stiffeners in terms of the coefficients F_{im} of the shear forces are substituted into equation (A10), a sufficient number of equations is obtained to give the coefficients F_{im} in terms of the coefficients a_n of the deflection function. In general, these equations are of the form

$$\sum_{j=1}^{N-1}\left(\delta_{ij} + \alpha_{ijm}\right)F_{jm} = EA_s\bar{z}_s\left(\frac{m\pi}{a}\right)^3\sum_{n=1}^{\infty} a_n \sin\frac{n\pi i}{N} \tag{A12}$$

$$(i = 1, 2, \ldots \infty)$$

where δ_{ij} is the Kronecker delta $\left(\delta_{ij} = 1 \text{ if } i = j; \quad \delta_{ij} = 0 \text{ if } i \neq j\right)$ and $\alpha_{ijm} = \alpha_{jim}$ and is given by the results of appendix B.

Determination of Stability Criterions

With the distribution of middle-surface forces and displacements in the buckled plate known in terms of the Fourier coefficients of the deflection function, the principle of minimum potential energy may be used to find the compressive buckling stress of the plate. The deflection function given by equation (A11) and the forces, strains, and displacements in terms of the coefficients of equation (A11) are substituted into the potential-energy expression for the structure. The

potential energy is then minimized with respect to each of the coefficients a_n. A set of simultaneous equations is obtained from which stability criterions can be determined.

The potential energy of an elastic body is defined as the difference between the strain energy of the body and the potential energy of applied edge loads. At the onset of instability the structure has potential energy due to the applied end loads which remains constant while the plate bends and need not be taken into consideration. After buckling the plate acquires additional strain energy which can be expressed as the sum of the strain energy of bending of the plate and the strain energy of deformations in the plane of the plate middle surface (ref. 10) as

$$
V_P = \frac{D}{2} \int_0^a \int_{-\frac{Nd}{2}}^{\frac{Nd}{2}} \left\{ \left(\nabla^2 w \right)^2 + 2(1 - \mu) \left[\left(\frac{\partial^2 w}{\partial x\, \partial y} \right)^2 - \frac{\partial^2 w}{\partial x^2} \frac{\partial^2 w}{\partial y^2} \right] \right\} dx\, dy -
$$

$$
\sum_{i=1}^N \int_0^a \int_{\left(i - \frac{N}{2} - 1\right)d}^{\left(i - \frac{N}{2}\right)d} \bar{\sigma}_x t \epsilon_{x_i}\, dx\, dy + \frac{1}{2} \sum_{i=1}^N \int_0^a \int_{\left(i - \frac{N}{2} - 1\right)d}^{\left(i - \frac{N}{2}\right)d} \left(N_{x_i} \epsilon_{x_i} + \right.
$$

$$
\left. N_{y_i} \epsilon_{y_i} + N_{xy_i} \gamma_{xy_i} \right) dx\, dy \tag{A13}
$$

The first term on the right-hand side of equation (A13) represents the strain energy of bending of the plate. The second term represents the strain energy arising from displacement of the middle-surface compressive forces, which remain constant as bending takes place, by additional stretching of the plate middle surface after buckling. The third term represents the strain energy due to stretching of the plate middle surface by the middle-surface forces that arise after buckling.

The additional potential energy of the compressive forces applied along the transverse edges of the plate is

$$
W_P = - \sum_{i=1}^N \int_{\left(i - \frac{N}{2} - 1\right)d}^{\left(i - \frac{N}{2}\right)d} \bar{\sigma}_x t \left[\left(u_i \right)_{x=a} - \left(u_i \right)_{x=0} \right] dy + \frac{\bar{\sigma}_x t}{2} \int_0^a \int_{-\frac{Nd}{2}}^{\frac{Nd}{2}} \left(\frac{\partial w}{\partial x} \right)^2 dx\, dy \tag{A14}
$$

The first term on the right-hand side of equation (A14) is the work done by the edge loads in moving through displacements due to the shear forces induced after buckling. The second term represents work done by the edge loads in moving through displacements due to bending. The form of this term is consistent with the assumption in small-deflection bending theory that the plate middle surface undergoes no stretching due to bending.

Similarly, the additional strain energy of the stiffeners is

$$V_S = \sum_{i=1}^{N-1} \frac{EI_S}{2} \int_0^a \left[\left(\frac{\partial^2 w}{\partial x^2}\right)_{y=\left(1-\frac{N}{2}\right)d} \right]^2 dx + \frac{1}{2} \sum_{i=1}^{N-1} \int_0^a P_i \epsilon_{S_i} \, dx - \sum_{i=1}^{N-1} \int_0^a \bar{\sigma}_x A_S \epsilon_{S_i} \, dx \qquad \text{(A15)}$$

and the additional potential energy of the end loads on the stiffeners is

$$W_S = -\sum_{i=1}^{N-1} \bar{\sigma}_x A_S \left[\left(u_{S_i}\right)_{x=a} - \left(u_{S_i}\right)_{x=0} \right] + \sum_{i=1}^{N-1} \frac{\bar{\sigma}_x A_S}{2} \int_0^a \left[\left(\frac{\partial w}{\partial x}\right)_{y=\left(1-\frac{N}{2}\right)d} \right]^2 dx \qquad \text{(A16)}$$

The total potential energy of the stiffened plate is then

$$U = V_P + V_S - W_P - W_S$$

$$= \frac{D}{2} \int_0^a \int_{-\frac{Nd}{2}}^{\frac{Nd}{2}} \left\{ (\nabla^2 w)^2 + 2(1-\mu)\left[\left(\frac{\partial^2 w}{\partial x \, \partial y}\right)^2 - \frac{\partial^2 w}{\partial x^2}\frac{\partial^2 w}{\partial y^2}\right] \right\} dx \, dy - \sum_{i=1}^{N} \int_0^a \int_{\left(1-\frac{N}{2}-1\right)d}^{\left(1-\frac{N}{2}\right)d} \bar{\sigma}_x t \epsilon_{x_i} \, dx \, dy +$$

$$\frac{1}{2} \sum_{i=1}^{N} \int_0^a \int_{\left(1-\frac{N}{2}-1\right)d}^{\left(1-\frac{N}{2}\right)d} \left(N_{x_i}\epsilon_{x_i} + N_{y_i}\epsilon_{y_i} + N_{xy_i}\gamma_{xy_i}\right) dx \, dy + \sum_{i=1}^{N-1} \frac{EI_S}{2} \int_0^a \left[\left(\frac{\partial^2 w}{\partial x^2}\right)_{y=\left(1-\frac{N}{2}\right)d}\right]^2 dx +$$

$$\frac{1}{2} \sum_{i=1}^{N-1} \int_0^a P_i \epsilon_{S_i} \, dx - \sum_{i=1}^{N-1} \int_0^a \bar{\sigma}_x A_S \epsilon_{S_i} \, dx + \sum_{i=1}^{N} \int_{\left(1-\frac{N}{2}-1\right)d}^{\left(1-\frac{N}{2}\right)d} \bar{\sigma}_x t \left[\left(u_i\right)_{x=a} - \left(u_i\right)_{x=0}\right] dy -$$

$$\frac{\bar{\sigma}_x t}{2} \int_0^a \int_{-\frac{Nd}{2}}^{\frac{Nd}{2}} \left(\frac{\partial w}{\partial x}\right)^2 dx \, dy + \sum_{i=1}^{N-1} \bar{\sigma}_x A_S \left[\left(u_{S_i}\right)_{x=a} - \left(u_{S_i}\right)_{x=0}\right] - \sum_{i=1}^{N-1} \frac{\bar{\sigma}_x A_S}{2} \int_0^a \left[\left(\frac{\partial w}{\partial x}\right)_{y=\left(1-\frac{N}{2}\right)d}\right]^2 dx \qquad \text{(A17)}$$

The potential-energy expression (eq. (A17)) can be considerably simplified by transforming some of the terms in the equation. Consider, for instance, the term representing the work done after buckling by the compressive forces applied to the plate in moving through displacements

due to the induced shear forces - that is, $\sum\limits_{i=1}^{N} \int_{\left(1-\frac{N}{2}-1\right)d}^{\left(1-\frac{N}{2}\right)d} \bar{\sigma}_x t \left[(u_i)_{x=a} - (u_i)_{x=0} \right] dy$. This term

can also be expressed as $\sum\limits_{i=1}^{N} \int_0^a \int_{\left(1-\frac{N}{2}-1\right)d}^{\left(1-\frac{N}{2}\right)d} \bar{\sigma}_x t \frac{\partial u_i}{\partial x} dx\, dy$ which is the equivalent of

$\sum\limits_{i=1}^{N} \int_0^a \int_{\left(1-\frac{N}{2}-1\right)d}^{\left(1-\frac{N}{2}\right)d} \bar{\sigma}_x t \epsilon_{x_i} dx\, dy$ and cancels the term representing the additional strain energy

in the plate arising from displacement of the constant middle-surface compressive forces after

buckling. Similarly, the term $\sum\limits_{i=1}^{N-1} \bar{\sigma}_x A_S \left[(u_{S_i})_{x=a} - (u_{S_i})_{x=0} \right]$ cancels $-\sum\limits_{i=1}^{N-1} \int_0^a \bar{\sigma}_x A_S \epsilon_{S_i} dx$.

The term representing the strain energy of stretching of the plate middle surface by the middle-surface forces that arise after buckling can be transformed to a much simpler expression by integrating the term by parts to obtain

$$\frac{1}{2}\sum_{i=1}^{N} \int_0^a \int_{\left(1-\frac{N}{2}-1\right)d}^{\left(1-\frac{N}{2}\right)d} \left(N_{x_i}\epsilon_{x_i} + N_{y_i}\epsilon_{y_i} + N_{xy_i}\gamma_{xy_i} \right)dx\,dy = \frac{1}{2}\sum_{i=1}^{N} \int_{\left(1-\frac{N}{2}-1\right)d}^{\left(1-\frac{N}{2}\right)d} \left[\left(N_{x_i}u_i\right)_{x=a} - \left(N_{x_i}u_i\right)_{x=0} \right] dy \,+$$

$$\frac{1}{2}\sum_{i=1}^{N} \int_0^a \left[\left(N_{y_i}v_i\right)_{y=\left(1-\frac{N}{2}\right)d} - \left(N_{y_i}v_i\right)_{y=\left(1-\frac{N}{2}-1\right)d} \right] dx + \frac{1}{2}\sum_{i=1}^{N} \int_0^a \left[\left(N_{xy_i}u_i\right)_{y=\left(1-\frac{N}{2}\right)d} - \left(N_{xy_i}u_i\right)_{y=\left(1-\frac{N}{2}-1\right)d} \right] dx \,+$$

$$\frac{1}{2}\sum_{i=1}^{N} \int_{\left(1-\frac{N}{2}-1\right)d}^{\left(1-\frac{N}{2}\right)d} \left[\left(N_{xy_i}v_i\right)_{x=a} - \left(N_{xy_i}v_i\right)_{x=0} \right] dy - \frac{1}{2}\sum_{i=1}^{N} \int_0^a \int_{\left(1-\frac{N}{2}-1\right)d}^{\left(1-\frac{N}{2}\right)d} \left[u_i\left(\frac{\partial N_{x_i}}{\partial x} + \frac{\partial N_{xy_i}}{\partial y}\right) + v_i\left(\frac{\partial N_{y_i}}{\partial y} + \frac{\partial N_{xy_i}}{\partial x}\right) \right] dx\,dy \quad (A18)$$

The first, second, fourth, and fifth integrals on the right-hand side
of equation (A18) vanish by virtue of the conditions at the plate edges
(eqs. (A4)), the equations of continuity along each contact line
(eqs. (A5)), and the equations of equilibrium of middle-surface forces
within each bay (eqs. (A1)). The third integral, however, has a value
and can be rewritten as

$$\frac{1}{2} \sum_{i=1}^{N} \int_0^a \left[\left(N_{xy_i} u_i\right)_{y=\left(i-\frac{N}{2}\right)d} - \left(N_{xy_i} u_i\right)_{y=\left(i-\frac{N}{2}-1\right)d} \right] dx =$$

$$\frac{1}{2} \int_0^a \left(N_{xy_N} u_N\right)_{y=\frac{Nd}{2}} dx + \frac{1}{2} \sum_{i=1}^{N-1} \int_0^a \left[\left(N_{xy_i} u_i\right) - \left(N_{xy_{i+1}} u_{i+1}\right) \right]_{y=\left(i-\frac{N}{2}\right)d} dx -$$

$$\frac{1}{2} \int_0^a \left(N_{xy_1} u_1\right)_{y=-\frac{Nd}{2}} dx \tag{A19}$$

But N_{xy_N} is zero at $y = \frac{Nd}{2}$ and N_{xy_1} is zero at $y = -\frac{Nd}{2}$ so that
the first and third integrals on the right-hand side of equation (A19)
vanish. Furthermore, when the conditions of equations (A5) are con-
sidered, the second integral can be rewritten as

$$\frac{1}{2} \sum_{i=1}^{N-1} \int_0^a F_i(u_i)_{y=\left(i-\frac{N}{2}\right)d} dx \tag{A20}$$

which is the transformed additional strain energy of deformation of the
plate middle surface. This result could also have been obtained by use
of the law of conservation of energy; that is, internal energy equals
external work.

In a similar manner, the following transformation can be obtained:

$$\frac{1}{2} \sum_{i=1}^{N-1} \int_0^a P_i \epsilon_{S_i} \, dx = -\frac{1}{2} \sum_{i=1}^{N-1} \int_0^a F_i u_{S_i} \, dx \tag{A21}$$

Equations (A20) and (A21) may be combined to yield

$$\frac{1}{2} \sum_{i=1}^{N-1} \int_0^a F_i \left[(u_i)_{y=\left(i-\frac{N}{2}\right)d} - u_{S_i} \right] dx \qquad (A22)$$

which, from the relationship given in equation (A10), can be written as

$$\frac{1}{2} \sum_{i=1}^{N-1} \int_0^a F_i \bar{z}_S \left(\frac{\partial w}{\partial x}\right)_{y=\left(i-\frac{N}{2}\right)d} dx \qquad (A23)$$

The simplified potential-energy expression is then

$$U = \frac{D}{2} \int_0^a \int_{-\frac{Nd}{2}}^{\frac{Nd}{2}} \left\{ (\nabla^2 w)^2 + 2(1-\mu)\left[\left(\frac{\partial^2 w}{\partial x \, \partial y}\right)^2 - \frac{\partial^2 w}{\partial x^2}\frac{\partial^2 w}{\partial y^2}\right] \right\} dx \, dy \; +$$

$$\sum_{i=1}^{N-1} \frac{EI_S}{2} \int_0^a \left[\left(\frac{\partial^2 w}{\partial x^2}\right)_{y=\left(i-\frac{N}{2}\right)d}\right]^2 dx + \frac{1}{2} \sum_{i=1}^{N-1} \int_0^a F_i \bar{z}_S \left(\frac{\partial w}{\partial x}\right)_{y=\left(i-\frac{N}{2}\right)d} dx \; -$$

$$\frac{\bar{\sigma}_x t}{2} \int_0^a \int_{-\frac{Nd}{2}}^{\frac{Nd}{2}} \left(\frac{\partial w}{\partial x}\right)^2 dx \, dy - \sum_{i=1}^{N-1} \frac{\bar{\sigma}_x A_S}{2} \int_0^a \left[\left(\frac{\partial w}{\partial x}\right)_{y=\left(i-\frac{N}{2}\right)d}\right]^2 dx \qquad (A24)$$

Substitution of the bending deflections w given by equation (A11) and the shear forces F_i given by equation (A9) into equation (A24) yields

$$\frac{8a^3}{m^4\pi^4NdD}\,U = \sum_{n=1}^{\infty}\left\{\left[1 + \frac{n^2}{N^2}\left(\frac{a/d}{m}\right)^2\right]^2 - \frac{d^2\bar{\sigma}_xt}{\pi^2D}\left(\frac{a/d}{m}\right)^2\right\}a_n^2 +$$

$$\frac{2}{N}\left[\frac{EI_S}{dD} - \frac{d^2\bar{\sigma}_xt}{\pi^2D}\left(\frac{a/d}{m}\right)^2\frac{A_S}{dt}\right]\sum_{i=1}^{N-1}\left(\sum_{n=1}^{\infty}a_n\sin\frac{n\pi i}{N}\right)^2 +$$

$$\frac{2}{N}\frac{EA_S\bar{z}_S^2}{dD}\sum_{i=1}^{N-1}\frac{F_{im}}{\left(\frac{m\pi}{a}\right)^3EA_S\bar{z}_S}\sum_{n=1}^{\infty}a_n\sin\frac{n\pi i}{N} \qquad\qquad (A25)$$

The third term on the right-hand side of equation (A25) is the contri-
bution to the potential energy of the structure of stretching of the
plate and stiffeners by the shear forces induced after buckling. If $\bar{z}_S$
were equal to zero, that is, if the center of gravity of each stiffener
cross section were at the middle surface of the plate, equation (A25)
would reduce to equation (A3) of reference 9.

Minimization of equation (A25) with respect to the coefficients a_n
yields

$$\left\{\left[1 + \frac{r^2}{N^2}\left(\frac{a/d}{m}\right)^2\right]^2 - \frac{d^2\bar{\sigma}_xt}{\pi^2D}\left(\frac{a/d}{m}\right)^2\right\}a_r +$$

$$\frac{2}{N}\left[\frac{EI_S}{dD} - \frac{d^2\bar{\sigma}_xt}{\pi^2D}\left(\frac{a/d}{m}\right)^2\frac{A_S}{dt}\right]\sum_{n=1}^{\infty}a_n\sum_{i=1}^{N-1}\sin\frac{r\pi i}{N}\sin\frac{n\pi i}{N} +$$

$$\frac{2}{N}\frac{EA_S\bar{z}_S^2}{dD}\sum_{i=1}^{N-1}\frac{1}{2}\left\{\frac{F_{im}}{\left(\frac{m\pi}{a}\right)^3EA_S\bar{z}_S}\sin\frac{r\pi i}{N} +\right.$$

$$\left.\frac{\partial}{\partial a_r}\left[\frac{F_{im}}{\left(\frac{m\pi}{a}\right)^3EA_S\bar{z}_S}\right]\sum_{n=1}^{\infty}a_n\sin\frac{n\pi i}{N}\right\} = 0 \qquad\qquad (A26)$$

$$(r = 1, 2, \ldots \infty)$$

When each coefficient F_{1m} is determined in terms of the coefficients a_n of the deflection function by the analysis of the preceding section and is substituted into equations (A26), the equations may then be manipulated to yield stability criterions for the stiffened plate. Since the expressions for F_{1m} differ for plates with different numbers of stiffeners, separate analyses are made in the following sections for a plate with one, two, three, or infinitely many stiffeners.

At this point it can be seen that the assumption of sinusoidal buckling in the longitudinal direction is justified. If sinusoidal buckling had not been assumed and an infinite number of longitudinal sine terms had been taken in equation (A11) for the deflection function (and, correspondingly, an infinite number of cosine terms in eqs. (A9) for the shear forces induced at each contact line), the terms corresponding to each sinusoidal component in the longitudinal direction would uncouple when the potential-energy expression was minimized and there would be obtained a different set of equations (A26) for each value of m. This uncoupling occurs only for the particular boundary condition chosen in the present paper; that is, points in the transverse edges of the plate are free to move in the y-direction before buckling occurs but are completely restrained from further movement after buckling.

Plate with one stiffener.- For a plate with one stiffener there is only one shear force induced in the plate - the one along the center line:

$$F_1 = F_{1m} \cos \frac{m\pi x}{a} \tag{A27}$$

The middle-surface displacements in the plate at the contact line due to this shear force are found from the appropriate equations for bay 1 and bay 2 derived in appendix B (eqs. (B13) or (B14)), with y and k set equal to zero and b replaced by $2d$, as

$$\left(u_1\right)_{y=0} = Z_{21}\left(\frac{a}{m\pi}\right)^2 \frac{F_{1m}}{Edt} \cos \frac{m\pi x}{a} \tag{A28}$$

where

$$Z_{21} = \frac{1}{4} \frac{(3 - \mu)(1 + \mu)\cosh \frac{2m\pi d}{a} + 2(1 + \mu)^2\left(\frac{m\pi d}{a}\right)^2 + 5 - 2\mu + \mu^2}{\sinh \frac{2m\pi d}{a} + \frac{2m\pi d}{a}} \frac{m\pi d}{a}$$

$$\tag{A29}$$

and the displacements in the stiffener at the contact line are, from equations (A10) and (B24),

$$u_{S_1} + \bar{z}_S \left(\frac{\partial w}{\partial x}\right)_{y=0} = -\left(\frac{a}{m\pi}\right)^2 \frac{F_{lm}}{EA_S} \cos\frac{m\pi x}{a} + \frac{m\pi}{a}\bar{z}_S \sum_{n=1}^{\infty} a_n \sin\frac{n\pi}{2}\cos\frac{m\pi x}{a}$$

$$(A30)$$

The condition that these two displacements are equal can then be written as

$$\left(1 + Z_{21}\frac{A_S}{dt}\right)\frac{F_{lm}}{\left(\frac{m\pi}{a}\right)^3 EA_S\bar{z}_S} = \sum_{n=1}^{\infty} a_n \sin\frac{n\pi}{2} \qquad (A31)$$

from which

$$\frac{F_{lm}}{\left(\frac{m\pi}{a}\right)^3 EA_S\bar{z}_S} = \frac{\displaystyle\sum_{n-1}^{\infty} a_n \sin\frac{n\pi}{2}}{1 + Z_{21}\frac{A_S}{dt}} \qquad (A32)$$

The substitution of equation (A32) into equations (A26), with N equal to 2, then yields

$$\left\{\left[1 + \frac{1}{4} r^2\left(\frac{a/d}{m}\right)^2\right]^2 - \frac{d^2\bar{\sigma}_x t}{\pi^2 D}\left(\frac{a/d}{m}\right)^2\right\} a_r +$$

$$\left[\frac{EI_S}{dD} + \frac{1}{1 + Z_{21}\frac{A_S}{dt}}\frac{EA_S\bar{z}_S^2}{dD} - \frac{d^2\bar{\sigma}_x t}{\pi^2 D}\left(\frac{a/d}{m}\right)^2\frac{A_S}{dt}\right]\sum_{n=1}^{\infty} a_n \sin\frac{r\pi}{2}\sin\frac{n\pi}{2} = 0$$

$$(A33)$$

$$(r = 1, 2, \ldots \infty)$$

Equations (A33) are practically identical with equations (A4) of reference 9 for $N = 2$, when those equations are divided by m^4, the only

difference being that the flexural-stiffness ratio (called γ in ref. 9) of equations (A4) is replaced in equations (A33) by an effective-flexural-stiffness ratio

$$\frac{EI_{eff}}{dD} = \frac{EI_S}{dD} + \frac{1}{1 + Z_{21}\frac{A_S}{dt}} \frac{EA_S \bar{z}_S^2}{dD} \tag{A34}$$

The criterions for buckling under uniform compression of a simply supported plate with one stiffener can therefore be written immediately from the results of reference 9 as follows:

For buckling of the plate with deflection of the stiffener,

$$\frac{EI_S}{dD} + \frac{1}{1 + Z_{21}\frac{A_S}{dt}} \frac{EA_S \bar{z}_S^2}{dD} = \frac{\frac{4}{\pi^2}\left(\frac{a/d}{m}\right)^3 \sqrt{\frac{d^2 \bar{\sigma}_x t}{\pi^2 D}}}{\frac{\tanh \theta_2}{\theta_2} - \frac{\tan \theta_1}{\theta_1}} + \frac{d^2 \bar{\sigma}_x t}{\pi^2 D}\left(\frac{a/d}{m}\right)^2 \frac{A_S}{dt} \tag{A35}$$

where

$$\theta_1 = \pi \sqrt{\frac{m}{a/d}\left(\sqrt{\frac{d^2 \bar{\sigma}_x t}{\pi^2 D}} - \frac{m}{a/d}\right)} \tag{A36a}$$

$$\theta_2 = \pi \sqrt{\frac{m}{a/d}\left(\sqrt{\frac{d^2 \bar{\sigma}_x t}{\pi^2 D}} + \frac{m}{a/d}\right)} \tag{A36b}$$

and, for buckling of the plate with a node at the stiffener,

$$\frac{d^2 \bar{\sigma}_x t}{\pi^2 D} = \left(\frac{m}{a/d} + p^2 \frac{a/d}{m}\right)^2 \tag{A37}$$

$$(p = 1, 2, \ldots \infty)$$

where p is the number of half-waves in the transverse direction in each bay. The lowest values of the buckling-stress parameter given by equation (A37) are obtained when p is set equal to 1.

Plate with two stiffeners.- For a plate with two stiffeners, two shear forces are induced in the plate:

Along the contact line at $y = -\frac{d}{2}$,

$$F_1 = F_{1m} \cos \frac{m\pi x}{a} \qquad \qquad \text{(A38a)}$$

and, along the contact line at $y = \frac{d}{2}$,

$$F_2 = F_{2m} \cos \frac{m\pi x}{a} \qquad \qquad \text{(A38b)}$$

The middle-surface displacements in the plate at each contact line due to these shear forces are obtained as follows: The shear force F_1 alone produces displacements u_1' along the contact line $y = -\frac{d}{2}$ which may be obtained from the appropriate equation for bay 1 and bay 2 of appendix B (eqs. (B13) or (B14)), with $k = -\frac{1}{3}$, $y = -\frac{1}{3}\frac{b}{2}$, and b replaced by $3d$, as

$$\left(u_1'\right)_{y=-\frac{d}{2}} = \frac{1}{2}\left(\frac{a}{m\pi}\right)^2\left(z_{31} + z_{32}\right)\frac{F_{1m}}{Edt} \cos \frac{m\pi x}{a} \qquad \text{(A39a)}$$

and displacements u_2' along the contact line $y = \frac{d}{2}$ which may be obtained from the displacement equation for bay 2 (eq. (B14)), with $k = -\frac{1}{3}$, $y = \frac{1}{3}\frac{b}{2}$, and b replaced by $3d$, as

$$\left(u_2'\right)_{y=\frac{d}{2}} = \frac{1}{2}\left(\frac{a}{m\pi}\right)^2\left(z_{31} - z_{32}\right)\frac{F_{1m}}{Edt} \cos \frac{m\pi x}{a} \qquad \text{(A39b)}$$

where

$$
Z_{31} = \frac{1}{4} \frac{m\pi d}{a} \frac{
\left\{
\begin{array}{l}
(3 - \mu)(1 + \mu)\left(\cosh \frac{3m\pi d}{a} + \cosh \frac{2m\pi d}{a} - \frac{2m\pi d}{a} \sinh \frac{m\pi d}{a}\right) + \\[2mm]
\left[5 - 2\mu + \mu^2 + 2(1 + \mu)^2\left(\frac{m\pi d}{a}\right)^2\right] \cosh \frac{m\pi d}{a} - \\[2mm]
(1 + \mu)^2 \frac{m\pi d}{a} \sinh \frac{2m\pi d}{a} + 5 - 2\mu + \mu^2 + 4(1 + \mu)^2\left(\frac{m\pi d}{a}\right)^2
\end{array}
\right\}
}{\sinh \frac{3m\pi d}{a} + \frac{3m\pi d}{a}}
$$

$$\text{(A40a)}$$

and

$$
Z_{32} = \frac{1}{4} \frac{m\pi d}{a} \frac{
\left\{
\begin{array}{l}
(3 - \mu)(1 + \mu)\left(\cosh \frac{3m\pi d}{a} - \cosh \frac{2m\pi d}{a} - \frac{2m\pi d}{a} \sinh \frac{m\pi d}{a}\right) + \\[2mm]
\left[5 - 2\mu + \mu^2 + 2(1 + \mu)^2\left(\frac{m\pi d}{a}\right)^2\right] \cosh \frac{m\pi d}{a} + \\[2mm]
(1 + \mu)^2 \frac{m\pi d}{a} \sinh \frac{2m\pi d}{a} - \left[5 - 2\mu + \mu^2 + 4(1 + \mu)^2\left(\frac{m\pi d}{a}\right)^2\right]
\end{array}
\right\}
}{\sinh \frac{3m\pi d}{a} - \frac{3m\pi d}{a}}
$$

$$\text{(A40b)}$$

Similarly, the shear force F_2 produces displacements u_1'' along the contact line $y = -\frac{d}{2}$

$$
\left(u_1''\right)_{y=-\frac{d}{2}} = \frac{1}{2}\left(\frac{a}{m\pi}\right)^2 (Z_{31} - Z_{32}) \frac{F_{2m}}{Edt} \cos \frac{m\pi x}{a}
\tag{A41a}
$$

and displacements u_2'' along the contact line $y = \frac{d}{2}$

$$
\left(u_2''\right)_{y=\frac{d}{2}} = \frac{1}{2}\left(\frac{a}{m\pi}\right)^2 (Z_{31} + Z_{32}) \frac{F_{2m}}{Edt} \cos \frac{m\pi x}{a}
\tag{A41b}
$$

The total displacements u_i along each contact line are obtained by adding the displacements $u_i{}'$ and $u_i{}''$ due to each of the forces and are

$$\left(u_1\right)_{y=-\frac{d}{2}} = \frac{1}{2}\left(\frac{a}{m\pi}\right)^2\left[\left(Z_{31} + Z_{32}\right)\frac{F_{1m}}{Edt} + \left(Z_{31} - Z_{32}\right)\frac{F_{2m}}{Edt}\right]\cos\frac{m\pi x}{a} \qquad \text{(A42a)}$$

$$\left(u_2\right)_{y=\frac{d}{2}} = \frac{1}{2}\left(\frac{a}{m\pi}\right)^2\left[\left(Z_{31} - Z_{32}\right)\frac{F_{1m}}{Edt} + \left(Z_{31} + Z_{32}\right)\frac{F_{2m}}{Edt}\right]\cos\frac{m\pi x}{a} \qquad \text{(A42b)}$$

The displacements in each stiffener at the contact line are

$$u_{S_1} + \bar{z}_S\left(\frac{\partial w}{\partial x}\right)_{y=-\frac{d}{2}} = -\left(\frac{a}{m\pi}\right)^2\frac{F_{1m}}{EA_S}\cos\frac{m\pi x}{a} + \frac{m\pi}{a}\bar{z}_S\sum_{n=1}^{\infty}a_n\sin\frac{n\pi}{3}\cos\frac{m\pi x}{a}$$

$$\text{(A43a)}$$

$$u_{S_2} + \bar{z}_S\left(\frac{\partial w}{\partial x}\right)_{y=\frac{d}{2}} = -\left(\frac{a}{m\pi}\right)^2\frac{F_{2m}}{EA_S}\cos\frac{m\pi x}{a} + \frac{m\pi}{a}\bar{z}_S\sum_{n=1}^{\infty}a_n\sin\frac{2n\pi}{3}\cos\frac{m\pi x}{a}$$

$$\text{(A43b)}$$

The conditions that the contact-line displacements in the plate and in the stiffeners are equal can be written as

$$\left[1+\frac{1}{2}\left(Z_{31}+Z_{32}\right)\frac{A_S}{dt}\right]\frac{F_{1m}}{\left(\frac{m\pi}{a}\right)^3 EA_S\bar{z}_S}+\frac{1}{2}\left(Z_{31}-Z_{32}\right)\frac{A_S}{dt}\frac{F_{2m}}{\left(\frac{m\pi}{a}\right)^3 EA_S\bar{z}_S} = \sum_{n=1}^{\infty}a_n\sin\frac{n\pi}{3}$$

$$\text{(A44a)}$$

$$\frac{1}{2}(Z_{31} - Z_{32})\frac{A_S}{dt} \frac{F_{1m}}{\left(\frac{m\pi}{a}\right)^3 EA_S\bar{z}_S} + \left[1 + \frac{1}{2}(Z_{31} + Z_{32})\frac{A_S}{dt}\right]\frac{F_{2m}}{\left(\frac{m\pi}{a}\right)^3 EA_S\bar{z}_S} = \sum_{n=1}^{\infty} a_n \sin\frac{2n\pi}{3}$$

$$(A44b)$$

from which the following relations are obtained:

$$\frac{F_{1m}}{\left(\frac{m\pi}{a}\right)^3 EA_S\bar{z}_S} = \frac{1}{2}\frac{1}{1 + Z_{31}\frac{A_S}{dt}}\sum_{n=1}^{\infty} a_n\left(\sin\frac{n\pi}{3} + \sin\frac{2n\pi}{3}\right) +$$

$$\frac{1}{2}\frac{1}{1 + Z_{32}\frac{A_S}{dt}}\sum_{n=1}^{\infty} a_n\left(\sin\frac{n\pi}{3} - \sin\frac{2n\pi}{3}\right) \qquad (A45a)$$

$$\frac{F_{2m}}{\left(\frac{m\pi}{a}\right)^3 EA_S\bar{z}_S} = \frac{1}{2}\frac{1}{1 + Z_{31}\frac{A_S}{dt}}\sum_{n=1}^{\infty} a_n\left(\sin\frac{n\pi}{3} + \sin\frac{2n\pi}{3}\right) -$$

$$\frac{1}{2}\frac{1}{1 + Z_{32}\frac{A_S}{dt}}\sum_{n=1}^{\infty} a_n\left(\sin\frac{n\pi}{3} - \sin\frac{2n\pi}{3}\right) \qquad (A45b)$$

Substitution of equations (A45) into equations (A26), with N equal to 3, then yields the following groups of equations:

For buckling symmetrical about the plate center line and with deflection of the stiffeners,

$$\left\{\left[1 + \left(2r + \frac{1}{3}\right)^2\left(\frac{a/d}{m}\right)^2\right]^2 - \frac{d^2\bar{\sigma}_x t}{\pi^2 D}\left(\frac{a/d}{m}\right)^2\right\}a_{6r+1} +$$

$$\left[\frac{EI_S}{dD} + \frac{1}{1 + Z_{31}\frac{A_S}{dt}}\frac{EA_S\bar{z}_S^2}{dD} - \frac{d^2\bar{\sigma}_x t}{\pi^2 D}\left(\frac{a/d}{m}\right)^2\frac{A_S}{dt}\right]\sum_{s=0}^{\infty}\left(a_{6s+1} - a_{6s+5}\right) = 0$$

$$(A46a)$$

$$(r = 0, 1, 2, \ldots \infty)$$

$$\left\{\left[1 + \left(2r + \frac{5}{3}\right)^2\left(\frac{a/d}{m}\right)^2\right]^2 - \frac{d^2\bar{\sigma}_x t}{\pi^2 D}\left(\frac{a/d}{m}\right)^2\right\}a_{6r+5} -$$

$$\left[\frac{EI_S}{dD} + \frac{1}{1 + Z_{31}\frac{A_S}{dt}}\frac{EA_S\bar{z}_S^2}{dD} - \frac{d^2\bar{\sigma}_x t}{\pi^2 D}\left(\frac{a/d}{m}\right)^2\frac{A_S}{dt}\right]\sum_{s=0}^{\infty}\left(a_{6s+1} - a_{6s+5}\right) = 0$$

$$(A46b)$$

$$(r = 0, 1, 2, \ldots \infty)$$

for buckling antisymmetrical about the plate center line and with deflection of the stiffeners,

$$\left\{\left[1 + \left(2r + \frac{2}{3}\right)^2\left(\frac{a/d}{m}\right)^2\right]^2 - \frac{d^2\bar{\sigma}_x t}{\pi^2 D}\left(\frac{a/d}{m}\right)^2\right\}a_{6r+2} +$$

$$\left[\frac{EI_S}{dD} + \frac{1}{1 + Z_{32}\frac{A_S}{dt}}\frac{EA_S\bar{z}_S^2}{dD} - \frac{d^2\bar{\sigma}_x t}{\pi^2 D}\left(\frac{a/d}{m}\right)^2\frac{A_S}{dt}\right]\sum_{s=0}^{\infty}\left(a_{6s+2} - a_{6s+4}\right) = 0$$

$$(A47a)$$

$$(r = 0, 1, 2, \ldots \infty)$$

$$\left\{\left[1 + \left(2r + \frac{4}{3}\right)^2\left(\frac{a/d}{m}\right)^2\right]^2 - \frac{d^2\bar{\sigma}_x t}{\pi^2 D}\left(\frac{a/d}{m}\right)^2\right\}a_{6r+4} -$$

$$\left[\frac{EI_S}{dD} + \frac{1}{1 + Z_{32}\frac{A_S}{dt}}\frac{EA_S\bar{z}_S^2}{dD} - \frac{d^2\bar{\sigma}_x t}{\pi^2 D}\left(\frac{a/d}{m}\right)^2\frac{A_S}{dt}\right]\sum_{s=0}^{\infty}\left(a_{6s+2} - a_{6s+4}\right) = 0$$

$$(A47b)$$

$$(r = 0, 1, 2, \ldots \infty)$$

and, for buckling with a node at each stiffener,

$$\left\{ \left[1 + p^2 \left(\frac{a/d}{m} \right)^2 \right]^2 - \frac{d^2 \bar{\sigma}_x t}{\pi^2 D} \left(\frac{a/d}{m} \right)^2 \right\} a_{3p} = 0 \qquad (A48)$$

$$(p = 1, 2, \ldots \infty)$$

Equations (A46) to (A48) are similar to those into which equations (A4) of reference 9 for $N = 3$ separate. The differences between the equations of the present paper and those of reference 9 are that, instead of the flexural-stiffness ratio γ, equations (A46) contain an effective-flexural-stiffness ratio

$$\frac{EI_{eff}}{dD} = \frac{EI_S}{dD} + \frac{1}{1 + Z_{31} \frac{A_S}{dt}} \frac{EA_S \bar{z}_S^2}{dD} \qquad (A49)$$

and equations (A47) contain an effective-flexural-stiffness ratio

$$\frac{EI_{eff}}{dD} = \frac{EI_S}{dD} + \frac{1}{1 + Z_{32} \frac{A_S}{dt}} \frac{EA_S \bar{z}_S^2}{dD} \qquad (A50)$$

The stability criterions can be written immediately from the results of reference 9 as follows:

For buckling symmetrical about the plate center line with deflection of the stiffeners,

$$\frac{EI_S}{dD} + \frac{1}{1 + Z_{31} \frac{A_S}{dt}} \frac{EA_S \bar{z}_S^2}{dD} = \frac{\frac{4}{\pi^2} \left(\frac{a/d}{m} \right)^3 \sqrt{\frac{d^2 \bar{\sigma}_x t}{\pi^2 D}}}{\dfrac{\dfrac{\sin \theta_1}{\theta_1}}{\dfrac{\sqrt{3}}{2} - \cos \theta_1} - \dfrac{\dfrac{\sinh \theta_2}{\theta_2}}{\dfrac{\sqrt{3}}{2} - \cosh \theta_2}} + \frac{d^2 \bar{\sigma}_x t}{\pi^2 D} \left(\frac{a/d}{m} \right)^2 \frac{A_S}{dt}$$

$$(A51)$$

for buckling antisymmetrical about the plate center line with deflection of the stiffeners,

$$
\frac{EI_S}{dD} + \frac{1}{1 + Z_{32}\frac{A_S}{dt}}\frac{EA_S\bar{z}_S{}^2}{dD} = \frac{\dfrac{4}{\pi^2}\left(\dfrac{a/d}{m}\right)^3\sqrt{\dfrac{d^2\bar{\sigma}_x t}{\pi^2 D}}}{\dfrac{\dfrac{\sinh\theta_2}{\theta_2}}{\dfrac{\sqrt{3}}{2}+\cosh\theta_2} - \dfrac{\dfrac{\sin\theta_1}{\theta_1}}{\dfrac{\sqrt{3}}{2}+\cos\theta_1}} + \frac{d^2\bar{\sigma}_x t}{\pi^2 D}\left(\frac{a/d}{m}\right)^2\frac{A_S}{dt}
$$

$$\tag{A52}$$

and, for buckling with a node at each stiffener,

$$
\frac{d^2\bar{\sigma}_x t}{\pi^2 D} = \left(\frac{m}{a/d} + p^2\,\frac{a/d}{m}\right)^2
\tag{A53}
$$

$$(p = 1, 2, \ldots \infty)$$

Plate with three stiffeners.- For a plate with three stiffeners, three shear forces must be considered:

Along the contact line $y = -d$,

$$
F_1 = F_{1m}\cos\frac{m\pi x}{a}
\tag{A54a}
$$

along the contact line $y = 0$,

$$
F_2 = F_{2m}\cos\frac{m\pi x}{a}
\tag{A54b}
$$

and, along the contact line $y = d$,

$$
F_3 = F_{3m}\cos\frac{m\pi x}{a}
\tag{A54c}
$$

The middle-surface displacements in the plate at each contact line are obtained from the displacement equations for bay 1 and bay 2 derived

in appendix B (eqs. (B13) and (B14)) by the procedure indicated in the preceding section as

$$\left(u_1\right)_{y=-d} = \left(\frac{a}{m\pi}\right)^2\left[\frac{1}{2}\left(\lambda_{1m} + \lambda_{2m}\right)\frac{F_{1m}}{Edt} + \lambda_{3m}\frac{F_{2m}}{Edt} + \frac{1}{2}\left(\lambda_{1m} - \lambda_{2m}\right)\frac{F_{3m}}{Edt}\right]\cos\frac{m\pi x}{a}$$

$$(A55a)$$

$$\left(u_2\right)_{y=0} = \left(\frac{a}{m\pi}\right)^2\left[\lambda_{3m}\frac{F_{1m}}{Edt} + \lambda_{4m}\frac{F_{2m}}{Edt} + \lambda_{3m}\frac{F_{3m}}{Edt}\right]\cos\frac{m\pi x}{a} \qquad (A55b)$$

$$\left(u_3\right)_{y=d} = \left(\frac{a}{m\pi}\right)^2\left[\frac{1}{2}\left(\lambda_{1m} - \lambda_{2m}\right)\frac{F_{1m}}{Edt} + \lambda_{3m}\frac{F_{2m}}{Edt} + \frac{1}{2}\left(\lambda_{1m} + \lambda_{2m}\right)\frac{F_{3m}}{Edt}\right]\cos\frac{m\pi x}{a}$$

$$(A55c)$$

where

$$\lambda_{1m} = \frac{1}{4}\frac{m\pi d}{a}\frac{\left\{\begin{array}{l}(3-\mu)(1+\mu)\left(\cosh\frac{4m\pi d}{a} + \cosh\frac{2m\pi d}{a} - \frac{2m\pi d}{a}\sinh\frac{2m\pi d}{a}\right) + \\[2mm] \left[5 - 2\mu + \mu^2 + 2(1+\mu)^2\left(\frac{m\pi d}{a}\right)^2\right]\cosh\frac{2m\pi d}{a} - \\[2mm] 2(1+\mu)^2\frac{m\pi d}{a}\sinh\frac{2m\pi d}{a} + 5 - 2\mu + \mu^2 + 6(1+\mu)^2\left(\frac{m\pi d}{a}\right)^2\end{array}\right\}}{\sinh\frac{4m\pi d}{a} + \frac{4m\pi d}{a}}$$

$$(A56a)$$

$$\lambda_{2m} = \frac{1}{4}\frac{m\pi d}{a}\frac{\left\{\begin{array}{l}(3-\mu)(1+\mu)\left(\cosh\frac{4m\pi d}{a} - \cosh\frac{2m\pi d}{a} - \frac{2m\pi d}{a}\sinh\frac{2m\pi d}{a}\right) + \\[2mm] \left[5 - 2\mu + \mu^2 + 2(1+\mu)^2\left(\frac{m\pi d}{a}\right)^2\right]\cosh\frac{2m\pi d}{a} + \\[2mm] 2(1+\mu)^2\frac{m\pi d}{a}\sinh\frac{2m\pi d}{a} - \left[5 - 2\mu + \mu^2 + 6(1+\mu)^2\left(\frac{m\pi d}{a}\right)^2\right]\end{array}\right\}}{\sinh\frac{4m\pi d}{a} - \frac{4m\pi d}{a}}$$

$$(A56b)$$

$$\lambda_{3m} = \frac{1}{4} \frac{m\pi d}{a} \frac{\left\{ (3-\mu)(1+\mu)\left(\cosh\frac{3m\pi d}{a} - \frac{3m\pi d}{a}\sinh\frac{m\pi d}{a}\right) + \left[5 - 2\mu + \mu^2 + 4(1+\mu)^2\left(\frac{m\pi d}{a}\right)^2\right]\cosh\frac{m\pi d}{a} - (1+\mu)^2\frac{m\pi d}{a}\sinh\frac{3m\pi d}{a} \right\}}{\sinh\frac{4m\pi d}{a} + \frac{4m\pi d}{a}}$$

$$\text{(A56c)}$$

$$\lambda_{4m} = \frac{1}{4} \frac{m\pi d}{a} \frac{(3-\mu)(1+\mu)\cosh\frac{4m\pi d}{a} + 8(1+\mu)^2\left(\frac{m\pi d}{a}\right)^2 + 5 - 2\mu + \mu^2}{\sinh\frac{4m\pi d}{a} + \frac{4m\pi d}{a}}$$

$$\text{(A56d)}$$

The displacements in the stiffeners are

$$u_{S_1} + \bar{z}_S\left(\frac{\partial w}{\partial x}\right)_{y=-d} = -\left(\frac{a}{m\pi}\right)^2 \frac{F_{1m}}{EA_S}\cos\frac{m\pi x}{a} + \frac{m\pi}{a}\bar{z}_S\sum_{n=1}^{\infty}a_n\sin\frac{n\pi}{4}\cos\frac{m\pi x}{a}$$

$$\text{(A57a)}$$

$$u_{S_2} + \bar{z}_S\left(\frac{\partial w}{\partial x}\right)_{y=0} = -\left(\frac{a}{m\pi}\right)^2 \frac{F_{2m}}{EA_S}\cos\frac{m\pi x}{a} + \frac{m\pi}{a}\bar{z}_S\sum_{n=1}^{\infty}a_n\sin\frac{n\pi}{2}\cos\frac{m\pi x}{a}$$

$$\text{(A57b)}$$

$$u_{S_3} + \bar{z}_S\left(\frac{\partial w}{\partial x}\right)_{y=d} = -\left(\frac{a}{m\pi}\right)^2 \frac{F_{3m}}{EA_S}\cos\frac{m\pi x}{a} + \frac{m\pi}{a}\bar{z}_S\sum_{n=1}^{\infty}a_n\sin\frac{3n\pi}{4}\cos\frac{m\pi x}{a}$$

$$\text{(A57c)}$$

The conditions that the contact-line displacements in the plate and in the stiffeners are equal then can be written as

$$\left[1 + \frac{1}{2}\left(\lambda_{1m} + \lambda_{2m}\right)\frac{A_S}{dt}\right]\frac{F_{1m}}{\left(\frac{m\pi}{a}\right)^3 EA_S \bar{z}_S} + \lambda_{3m}\frac{A_S}{dt}\frac{F_{2m}}{\left(\frac{m\pi}{a}\right)^3 EA_S \bar{z}_S} +$$

$$\frac{1}{2}\left(\lambda_{1m} - \lambda_{2m}\right)\frac{A_S}{dt}\frac{F_{3m}}{\left(\frac{m\pi}{a}\right)^3 EA_S \bar{z}_S} = \sum_{n=1}^{\infty} a_n \sin\frac{n\pi}{4} \qquad (A58a)$$

$$\lambda_{3m}\frac{A_S}{dt}\frac{F_{1m}}{\left(\frac{m\pi}{a}\right)^3 EA_S \bar{z}_S} + \left(1 + \lambda_{4m}\right)\frac{A_S}{dt}\frac{F_{2m}}{EA_S \bar{z}_S \left(\frac{m\pi}{a}\right)^3} +$$

$$\lambda_{3m}\frac{A_S}{dt}\frac{F_{3m}}{\left(\frac{m\pi}{a}\right)^3 EA_S \bar{z}_S} = \sum_{n=1}^{\infty} a_n \sin\frac{n\pi}{2} \qquad (A58b)$$

$$\frac{1}{2}\left(\lambda_{1m} - \lambda_{2m}\right)\frac{A_S}{dt}\frac{F_{1m}}{\left(\frac{m\pi}{a}\right)^3 EA_S \bar{z}_S} + \lambda_{3m}\frac{F_{2m}}{\left(\frac{m\pi}{a}\right)^3 EA_S \bar{z}_S} +$$

$$\left[1 + \frac{1}{2}\left(\lambda_{1m} + \lambda_{2m}\right)\frac{A_S}{dt}\right]\frac{F_{3m}}{\left(\frac{m\pi}{a}\right)^3 EA_S \bar{z}_S} = \sum_{n=1}^{\infty} a_n \sin\frac{n\pi}{3} \qquad (A58c)$$

from which are obtained

$$
\frac{F_{1m}}{\left(\frac{m\pi}{a}\right)^3 EA_S \bar{z}_S} = \frac{1}{2}\left[\frac{1 + \lambda_{4m}\frac{A_S}{dt} \cdot}{\left(1 + \lambda_{1m}\frac{A_S}{dt}\right)\left(1 + \lambda_{4m}\frac{A_S}{dt}\right) - 2\left(\lambda_{3m}\frac{A_S}{dt}\right)^2} \sum_{n=1}^{\infty} a_n\left(\sin\frac{n\pi}{4} + \sin\frac{3n\pi}{4}\right) - \right.
$$

$$
\frac{2\lambda_{3m}\frac{A_S}{dt}}{\left(1 + \lambda_{1m}\frac{A_S}{dt}\right)\left(1 + \lambda_{4m}\frac{A_S}{dt}\right) - 2\left(\lambda_{3m}\frac{A_S}{dt}\right)^2} \sum_{n=1}^{\infty} a_n \sin\frac{n\pi}{2} +
$$

$$
\left. \frac{1}{1 + \lambda_{2m}\frac{A_S}{dt}} \sum_{n=1}^{\infty} a_n\left(\sin\frac{n\pi}{4} - \sin\frac{3n\pi}{4}\right) \right] \tag{A59a}
$$

$$
\frac{F_{2m}}{\left(\frac{m\pi}{a}\right)^3 EA_S \bar{z}_S} = - \frac{\lambda_{3m}\frac{A_S}{dt}}{\left(1 + \lambda_{1m}\frac{A_S}{dt}\right)\left(1 + \lambda_{4m}\frac{A_S}{dt}\right) - 2\left(\lambda_{3m}\frac{A_S}{dt}\right)^2} \sum_{n=1}^{\infty} a_n\left(\sin\frac{n\pi}{4} + \sin\frac{3n\pi}{4}\right) +
$$

$$
\frac{1 + \lambda_{1m}\frac{A_S}{dt}}{\left(1 + \lambda_{1m}\frac{A_S}{dt}\right)\left(1 + \lambda_{4m}\frac{A_S}{dt}\right) - 2\left(\lambda_{3m}\frac{A_S}{dt}\right)^2} \sum_{n=1}^{\infty} a_n \sin\frac{n\pi}{2} \tag{A59b}
$$

$$
\frac{F_{3m}}{\left(\frac{m\pi}{a}\right)^3 EA_S \bar{z}_S} = -\frac{1}{2}\left[-\frac{1 + \lambda_{4m}\frac{A_S}{dt}}{\left(1 + \lambda_{1m}\frac{A_S}{dt}\right)\left(1 + \lambda_{4m}\frac{A_S}{dt}\right) - 2\left(\lambda_{3m}\frac{A_S}{dt}\right)^2} \sum_{n=1}^{\infty} a_n\left(\sin\frac{n\pi}{4} + \sin\frac{3n\pi}{4}\right) + \right.
$$

$$
\frac{2\lambda_{3m}\frac{A_S}{dt}}{\left(1 + \lambda_{1m}\frac{A_S}{dt}\right)\left(1 + \lambda_{4m}\frac{A_S}{dt}\right) - 2\left(\lambda_{3m}\frac{A_S}{dt}\right)^2} \sum_{n=1}^{\infty} a_n \sin\frac{n\pi}{2} +
$$

$$
\left. \frac{1}{1 + \lambda_{2m}\frac{A_S}{dt}} \sum_{n=1}^{\infty} a_n\left(\sin\frac{n\pi}{4} - \sin\frac{3n\pi}{4}\right) \right] \tag{A59c}
$$

After equations (A59) are substituted into equations (A26) the following groups of equations are obtained:

For buckling symmetrical about the longitudinal center line of the plate,

$$\left\{\left[1 + \left(2r + \frac{1}{4}\right)^2\left(\frac{a/d}{m}\right)^2\right]^2 - \frac{d^2\bar{\sigma}_x t}{\pi^2 D}\left(\frac{a/d}{m}\right)^2\right\}a_{8r+1} +$$

$$\left[\frac{EI_S}{dD} + \frac{1 + \left(\frac{\lambda_{1m} + \lambda_{4m}}{2} - \sqrt{2}\lambda_{3m}\right)\frac{A_S}{dt}}{\left(1 + \lambda_{1m}\frac{A_S}{dt}\right)\left(1 + \lambda_{4m}\frac{A_S}{dt}\right) - 2\left(\lambda_{3m}\frac{A_S}{dt}\right)^2}\frac{EA_S\bar{z}_S^2}{dD} - \right.$$

$$\left.\frac{d^2\bar{\sigma}_x t}{\pi^2 D}\left(\frac{a/d}{m}\right)^2\frac{A_S}{dt}\right]\sum_{s=0}^{\infty}\left(a_{8s+1} - a_{8s+7}\right) -$$

$$\frac{\frac{\lambda_{1m} - \lambda_{4m}}{2}\frac{A_S}{dt}}{\left(1 + \lambda_{1m}\frac{A_S}{dt}\right)\left(1 + \lambda_{4m}\frac{A_S}{dt}\right) - 2\left(\lambda_{3m}\frac{A_S}{dt}\right)^2}\frac{EA_S\bar{z}_S^2}{dD}\sum_{s=0}^{\infty}\left(a_{8s+3} - a_{8s+5}\right) = 0 \qquad \text{(A60a)}$$

$$(r = 0, 1, 2, \ldots \infty)$$

$$\left\{\left[1 + \left(2r + \frac{7}{4}\right)^2\left(\frac{a/d}{m}\right)^2\right]^2 - \frac{d^2\bar{\sigma}_x t}{\pi^2 D}\left(\frac{a/d}{m}\right)^2\right\}a_{8r+7} -$$

$$\left[\frac{EI_S}{dD} + \frac{1 + \left(\frac{\lambda_{1m} + \lambda_{4m}}{2} - \sqrt{2}\lambda_{3m}\right)\frac{A_S}{dt}}{\left(1 + \lambda_{1m}\frac{A_S}{dt}\right)\left(1 + \lambda_{4m}\frac{A_S}{dt}\right) - 2\left(\lambda_{3m}\frac{A_S}{dt}\right)^2}\frac{EA_S\bar{z}_S^2}{dD} - \right.$$

$$\left.\frac{d^2\bar{\sigma}_x t}{\pi^2 D}\left(\frac{a/d}{m}\right)^2\frac{A_S}{dt}\right]\sum_{s=0}^{\infty}\left(a_{8s+1} - a_{8s+7}\right) +$$

$$\frac{\left(\frac{\lambda_{1m} - \lambda_{4m}}{2}\right)\frac{A_S}{dt}}{\left(1 + \lambda_{1m}\frac{A_S}{dt}\right)\left(1 + \lambda_{4m}\frac{A_S}{dt}\right) - 2\left(\lambda_{3m}\frac{A_S}{dt}\right)^2}\frac{EA_S\bar{z}_S^2}{dD}\sum_{s=0}^{\infty}\left(a_{8s+3} - a_{8s+5}\right) = 0 \qquad \text{(A60b)}$$

$$(r = 0, 1, 2, \ldots \infty)$$

$$\left\{\left[1 + \left(2r + \frac{3}{4}\right)^2\left(\frac{a/d}{m}\right)^2\right]^2 - \frac{d^2\bar{\sigma}_x t}{\pi^2 D}\left(\frac{a/d}{m}\right)^2\right\}a_{8r+3} +$$

$$\left[\frac{EI_S}{dD} + \frac{1 + \left(\frac{\lambda_{1m} + \lambda_{4m}}{2} + \sqrt{2}\lambda_{3m}\right)\frac{A_S}{dt}}{\left(1 + \lambda_{1m}\frac{A_S}{dt}\right)\left(1 + \lambda_{4m}\frac{A_S}{dt}\right) - 2\left(\lambda_{3m}\frac{A_S}{dt}\right)^2}\frac{EA_S\bar{z}_S^2}{dD} - \right.$$

$$\left.\frac{d^2\bar{\sigma}_x t}{\pi^2 D}\left(\frac{a/d}{m}\right)^2\frac{A_S}{dt}\right]\sum_{s=0}^{\infty}\left(a_{8s+3} - a_{8s+5}\right) -$$

$$\frac{\left(\frac{\lambda_{1m} - \lambda_{4m}}{2}\right)\frac{A_S}{dt}}{\left(1 + \lambda_{1m}\frac{A_S}{dt}\right)\left(1 + \lambda_{4m}\frac{A_S}{dt}\right) - 2\left(\lambda_{3m}\frac{A_S}{dt}\right)^2}\frac{EA_S\bar{z}_S^2}{dD}\sum_{s=0}^{\infty}\left(a_{8s+1} - a_{8s+7}\right) = 0 \quad (A60c)$$

$$(r = 0, 1, 2, \ldots \infty)$$

$$\left\{\left[1 + \left(2r + \frac{5}{4}\right)^2\left(\frac{a/d}{m}\right)^2\right]^2 - \frac{d^2\bar{\sigma}_x t}{\pi^2 D}\left(\frac{a/d}{m}\right)^2\right\}a_{8r+5} -$$

$$\left[\frac{EI_S}{dD} + \frac{1 + \left(\frac{\lambda_{1m} + \lambda_{4m}}{2} - \sqrt{2}\lambda_{3m}\right)\frac{A_S}{dt}}{\left(1 + \lambda_{1m}\frac{A_S}{dt}\right)\left(1 + \lambda_{4m}\frac{A_S}{dt}\right) - 2\left(\lambda_{3m}\frac{A_S}{dt}\right)^2}\frac{EA_S\bar{z}_S^2}{dD} - \right.$$

$$\left.\frac{d^2\bar{\sigma}_x t}{\pi^2 D}\left(\frac{a/d}{m}\right)^2\frac{A_S}{dt}\right]\sum_{s=0}^{\infty}\left(a_{8s+3} - a_{8s+5}\right) +$$

$$\frac{\left(\frac{\lambda_{1m} - \lambda_{4m}}{2}\right)\frac{A_S}{dt}}{\left(1 + \lambda_{1m}\frac{A_S}{dt}\right)\left(1 + \lambda_{4m}\frac{A_S}{dt}\right) - 2\left(\lambda_{3m}\frac{A_S}{dt}\right)^2}\frac{EA_S\bar{z}_S^2}{dD}\sum_{s=0}^{\infty}\left(a_{8s+1} - a_{8s+7}\right) = 0 \quad (A60d)$$

$$(r = 0, 1, 2, \ldots \infty)$$

for buckling antisymmetrical about the longitudinal center line of the plate,

$$\left\{\left[1 + \left(2r + \frac{1}{2}\right)^2\left(\overline{\frac{a/d}{m}}\right)^2\right]^2 - \frac{d^2\bar{\sigma}_x t}{\pi^2 D}\left(\frac{a/d}{m}\right)^2\right\} a_{8r+2} +$$

$$\left[\frac{EI_S}{dD} + \frac{1}{1 + \lambda_{2m}\frac{A_S}{dt}}\frac{EA_S \bar{z}_S^2}{dD} - \frac{d^2\bar{\sigma}_x t}{\pi^2 D}\left(\frac{a/d}{m}\right)^2 \frac{A_S}{dt}\right]\sum_{s=0}^{\infty}\left(a_{8s+2} - a_{8s+6}\right) = 0$$

$$(A61a)$$

$$(r = 0,\ 1,\ 2,\ \ldots\ \infty)$$

$$\left\{\left[1 + \left(2r + \frac{3}{2}\right)^2\left(\overline{\frac{a/d}{m}}\right)^2\right]^2 - \frac{d^2\bar{\sigma}_x t}{\pi^2 D}\left(\frac{a/d}{m}\right)^2\right\} a_{8r+6} -$$

$$\left[\frac{EI_S}{dD} + \frac{1}{1 + \lambda_{2m}\frac{A_S}{dt}}\frac{EA_S \bar{z}_S^2}{dD} - \frac{d^2\bar{\sigma}_x t}{\pi^2 D}\left(\frac{a/d}{m}\right)^2 \frac{A_S}{dt}\right]\sum_{s=0}^{\infty}\left(a_{8s+2} - a_{8s+6}\right) = 0$$

$$(A61b)$$

$$(r = 0,\ 1,\ 2,\ \ldots\ \infty)$$

and, for buckling with a node along each stiffener,

$$\left\{\left[1 + p^2\left(\overline{\frac{a/d}{m}}\right)^2\right]^2 - \frac{d^2\bar{\sigma}_x t}{\pi^2 D}\left(\frac{a/d}{m}\right)^2\right\} a_{4p} = 0 \qquad (A62)$$

$$(p = 1,\ 2,\ \ldots\ \infty)$$

A comparison of equations (A60) and (A61) with equations (A4) of reference 9 indicates that equations (A61) differ from the corresponding equations (A4) only by the substitution of an effective-flexural-stiffness ratio

$$\frac{EI_{eff}}{dD} = \frac{EI_S}{dD} + \frac{1}{1 + \lambda_{2m}\dfrac{A_S}{dt}}\,\frac{EA_S\bar{z}_S^{\,2}}{dD} \tag{A63}$$

for the flexural-stiffness ratio γ. Equations (A60), however, differ radically from the corresponding equations (A4) of reference 9 in that those equations containing deflection-function coefficients of the form a_{8s+1} and a_{8s+7} are not independent of those containing deflection-function coefficients of the form a_{8s+3} and a_{8s+5}. A single criterion for buckling symmetrical about the longitudinal center line of the plate is thus obtained rather than two criterions corresponding to those of reference 9. Application of the method of solution of reference 11 and the results of reference 9 yields the following criterions:

For buckling symmetrical about the longitudinal center line of the plate,

$$
\left[\frac{EI_S}{dD} + \frac{1 + \left(\dfrac{\lambda_{1m}+\lambda_{4m}}{2} - \sqrt{2}\,\lambda_{3m}\right)\dfrac{A_S}{dt}}{\left(1+\lambda_{1m}\dfrac{A_S}{dt}\right)\left(1+\lambda_{4m}\dfrac{A_S}{dt}\right) - 2\left(\lambda_{3m}\dfrac{A_S}{dt}\right)^2}\,\frac{EA_S\bar{z}_S^{\,2}}{dD} - \frac{\dfrac{4}{\pi^2}\left(\dfrac{a/d}{m}\right)^3\sqrt{\dfrac{d^2\bar{\sigma}_x t}{\pi^2 D}}}{\dfrac{\sin\theta_1/\theta_1}{\dfrac{\sqrt2}{2}-\cos\theta_1} - \dfrac{\sinh\theta_2/\theta_2}{\dfrac{\sqrt2}{2}-\cosh\theta_2}}\right]
$$

$$
\times\;\frac{d^2\bar{\sigma}_x t}{\pi^2 D}\left(\frac{a/d}{m}\right)^2\frac{A_S}{dt}\left[\frac{EI_S}{dD} + \frac{1 + \left(\dfrac{\lambda_{1m}+\lambda_{4m}}{2} + \sqrt{2}\,\lambda_{3m}\right)\dfrac{A_S}{dt}}{\left(1+\lambda_{1m}\dfrac{A_S}{dt}\right)\left(1+\lambda_{4m}\dfrac{A_S}{dt}\right) - 2\left(\lambda_{3m}\dfrac{A_S}{dt}\right)^2}\,\frac{EA_S\bar{z}_S^{\,2}}{dD} - \frac{\dfrac{4}{\pi^2}\left(\dfrac{a/d}{m}\right)^3\sqrt{\dfrac{d^2\bar{\sigma}_x t}{\pi^2 D}}}{\dfrac{\sinh\theta_2/\theta_2}{\dfrac{\sqrt2}{2}+\cosh\theta_2} - \dfrac{\sin\theta_1/\theta_1}{\dfrac{\sqrt2}{2}+\cos\theta_1}}\right]
$$

$$
-\;\frac{d^2\bar{\sigma}_x t}{\pi^2 D}\left(\frac{a/d}{m}\right)^2\frac{A_S}{dt} - \left[\frac{\left(\dfrac{\lambda_{1m}-\lambda_{4m}}{2}\right)\dfrac{A_S}{dt}}{\left(1+\lambda_{1m}\dfrac{A_S}{dt}\right)\left(1+\lambda_{4m}\dfrac{A_S}{dt}\right) - 2\left(\lambda_{3m}\dfrac{A_S}{dt}\right)^2}\,\frac{EA_S\bar{z}_S^{\,2}}{dD}\right]^2 = 0 \tag{A64}
$$

for buckling antisymmetrical about the longitudinal center line of the plate,

$$\frac{EI_S}{dD} + \frac{1}{1 + \lambda_{2m}\frac{A_S}{dt}}\frac{EA_S\bar{z}_S^2}{dD} = \frac{\frac{4}{\pi^2}\left(\frac{a/d}{m}\right)^3\sqrt{\frac{d^2\bar{\sigma}_x t}{\pi^2 D}}}{\frac{\tanh\theta_2}{\theta_2} - \frac{\tan\theta_1}{\theta_1}} + \frac{d^2\bar{\sigma}_x t}{\pi^2 D}\left(\frac{a/d}{m}\right)^2\frac{A_S}{dt} \qquad (A65)$$

and, for buckling with a longitudinal node at each stiffener,

$$\frac{d^2\bar{\sigma}_x t}{\pi^2 D} = \left(\frac{m}{a/d} + p^2\frac{a/d}{m}\right)^2 \qquad (p = 1, 2, \ldots \infty) \qquad (A66)$$

It is noted that, when $\bar{z}_S$ is equal to zero, equation (A64) yields the two stability criterions for symmetrical buckling given in reference 9, that is, equations (A7) of that reference for $\frac{q}{N} = \frac{1}{4}$ and $\frac{q}{N} = \frac{3}{4}$.

Plate with infinitely many stiffeners.- As the number of stiffeners is increased the work involved in obtaining stability criterions becomes greater and the stability criterions become very much more complex. A complete investigation of all the possible modes of buckling of a plate with infinitely many stiffeners is therefore out of the question. The investigations in this section are limited to that mode of buckling in which the deflected shape of each bay of the plate is identical with that of the others, since the numerical results of reference 9 indicate that this mode of buckling is predominant for a plate with infinitely many stiffeners. The deflected shape of the plate in the transverse direction is considered to be of the form shown in figure 5(a), symmetrical about the center line of each bay and horizontal tangents at each stiffener. The equation of the deflection surface can then be expressed as

$$w = \sin\frac{m\pi x}{a}\sum_{n=0}^{\infty}a_n\cos\frac{2n\pi y}{d} \qquad (A67)$$

The shear forces induced after buckling are identical at each contact line and are distributed between adjacent bays of the plate as shown in figure 5(b), half of the force being applied to one bay and the other half to the adjacent bay.

Only part of the buckled plate, the part between the center line of one bay and the center line of an adjacent bay, need be considered since the deflected shape is periodic. The potential energy of this part of the plate can be written as

$$U = \frac{D}{2} \int_0^a \int_{-\frac{d}{2}}^{\frac{d}{2}} \left\{ \left(\nabla^2 w\right)^2 + 2(1 - \mu)\left[\left(\frac{\partial^2 w}{\partial x\, \partial y}\right)^2 - \frac{\partial^2 w}{\partial x^2}\frac{\partial^2 w}{\partial y^2}\right]\right\} dx\, dy +$$

$$\frac{EI_S}{dD} \int_0^a \left[\left(\frac{\partial^2 w}{\partial x^2}\right)_{y=0}\right]^2 dx + \frac{1}{2} \int_0^a F_\infty \bar{z}_S \left(\frac{\partial w}{\partial x}\right)_{y=0} dx -$$

$$\frac{\bar{\sigma}_x t}{2} \int_0^a \int_{-\frac{d}{2}}^{\frac{d}{2}} \left(\frac{\partial w}{\partial x}\right)^2 dx\, dy - \frac{\bar{\sigma}_x A_S}{2} \int_0^a \left[\left(\frac{\partial w}{\partial x}\right)_{y=0}\right]^2 dx \qquad (A68)$$

where F_∞ is the shear force induced after buckling.

If F_∞ is taken in the form

$$F_\infty = F_m' \cos \frac{m\pi x}{a} \qquad (A69)$$

the displacements u_m' in the plate at the contact line are derived in appendix B (see eq. (B20)) as

$$\left(u_m'\right)_{y=0} = \frac{1 + \mu}{4} \frac{(3 - \mu)\sinh \frac{m\pi d}{a} - (1 + \mu)\frac{m\pi d}{a}}{\cosh \frac{m\pi d}{a} - 1} \frac{a}{m\pi}\frac{F_m'}{Et} \cos \frac{m\pi x}{a} \qquad (A70)$$

and the displacements u_S' in the stiffener at the contact line are

$$u_S' + \bar{z}_S\left(\frac{\partial w}{\partial x}\right)_{y=0} = -\left(\frac{a}{m\pi}\right)^2 \frac{F_m'}{EA_S} \cos\frac{m\pi x}{a} + \frac{m\pi}{a}\bar{z}_S \sum_{n=0}^{\infty} a_n \cos\frac{m\pi x}{a} \qquad (A71)$$

The condition that these two displacements are equal yields

$$\frac{F_m'}{\left(\frac{m\pi}{a}\right)^3 EA_S\bar{z}_S} = \frac{\displaystyle\sum_{n=0}^{\infty} a_n}{1 + \dfrac{1+\mu}{4}\dfrac{(3-\mu)\sinh\dfrac{m\pi d}{a} - (1+\mu)\dfrac{m\pi d}{a}}{\cosh\dfrac{m\pi d}{a} - 1}\dfrac{m\pi d}{a}\dfrac{A_S}{dt}} \qquad (A72)$$

Substitution of equations (A67) and (A72) into the potential-energy expression (eq. (A68)) and minimization of the resultant expression with respect to the deflection-function coefficients a_n then yields the equations

$$\left\{\left[1 + 4r^2\left(\frac{a/d}{m}\right)^{\overline{2}}\right]^2 (1 + \delta_{r0}) - \frac{d^2\bar{\sigma}_x t}{\pi^2 D}\left(\frac{a/d}{m}\right)^2\right\}a_r +$$

$$\left[\frac{EI_S}{dD} + \frac{1}{1 + \dfrac{1+\mu}{4}\dfrac{(3-\mu)\sinh\dfrac{m\pi d}{a} - (1+\mu)\dfrac{m\pi d}{a}}{\cosh\dfrac{m\pi d}{a} - 1}\dfrac{m\pi d}{a}\dfrac{A_S}{dt}} \frac{EA_S\bar{z}_S^2}{dD} - \right.$$

$$\left. \frac{d^2\bar{\sigma}_x t}{\pi^2 D}\left(\frac{a/d}{m}\right)^2\frac{A_S}{dt}\right]\sum_{n=0}^{\infty} a_n = 0 \qquad (r = 0,\ 1,\ 2,\ \ldots\ \infty) \qquad (A73)$$

where δ_{r0} is the Kronecker delta $\left(\delta_{r0} = 1 \text{ if } r = 0 \text{ and } \delta_{r0} = 0 \text{ if } r \neq 0\right)$.

When the method of reference 11 is used to manipulate equations (A73) and the results of reference 9 are used, the following stability criterion is obtained:

$$\frac{EI_S}{dD} + \cfrac{1}{1 + \cfrac{1 + \mu}{4} \cfrac{(3 - \mu)\sinh\frac{m\pi d}{a} - (1 + \mu)\frac{m\pi d}{a}}{\cosh\frac{m\pi d}{a} - 1} \frac{m\pi d}{a} \frac{A_S}{dt}} \frac{EA_S\bar{z}_S^2}{dD} =$$

$$\frac{\cfrac{4}{\pi^2}\left(\frac{a/d}{m}\right)^3 \sqrt{\cfrac{d^2\bar{\sigma}_x t}{\pi^2 D}}}{\cfrac{\cot\frac{1}{2}\theta_1}{\theta_1} - \cfrac{\coth\frac{1}{2}\theta_2}{\theta_2}} + \frac{d^2\bar{\sigma}_x t}{\pi^2 D}\left(\frac{a/d}{m}\right)^2 \frac{A_S}{dt} \tag{A74}$$

This equation is, except for the flexural-stiffness ratio γ being replaced by an effective-flexural-stiffness ratio

$$\frac{EI_{eff}}{dD} = \frac{EI_S}{dD} + \cfrac{1}{1 + \cfrac{1 + \mu}{4} \cfrac{(3 - \mu)\sinh\frac{m\pi d}{a} - (1 + \mu)\frac{m\pi d}{a}}{\cosh\frac{m\pi d}{a} - 1} \frac{m\pi d}{a} \frac{A_S}{dt}} \frac{EA_S\bar{z}_S^2}{dD} \tag{A75}$$

identical to equation (A7) of reference 9 for $\frac{q}{N}$ equal to zero.

The terms in the deflection function that yield the stability criterion for buckling with longitudinal nodes along each stiffener have not been included in the investigation of plates with infinitely many stiffeners. This criterion should be considered, however, and is given as before by

$$\frac{d^2\bar{\sigma}_x t}{\pi^2 D} = \left(\frac{m}{a/d} + p^2\frac{a/d}{m}\right)^2 \qquad (p = 1, 2, \ldots \infty) \tag{A76}$$

APPENDIX B

MIDDLE-SURFACE FORCES AND DISPLACEMENTS DUE TO SHEAR FORCES

APPLIED ALONG A LONGITUDINAL LINE IN THE PLATE

Plate of Finite Width

Consider a plate subjected to an arbitrarily placed middle-surface shearing force of the form

$$F = F_m \cos \frac{m\pi x}{a} \tag{B1}$$

along the line $y = k \frac{b}{2}$. (See fig. 6.) This force divides the plate into two bays. Within each bay of the plate, middle-surface forces and displacements are continuous and are related by equations (A1) to (A3). At the line of application of the shear force, however, middle-surface shear forces are discontinuous and forces and displacements of the two bays are related by equations (A5). It is convenient to introduce a force function ϕ_j for each bay, such that

$$\left.\begin{array}{l} N_{x_{jm}} = \dfrac{\partial^2 \phi_{jm}}{\partial y^2} \\[4mm] N_{y_{jm}} = \dfrac{\partial^2 \phi_{jm}}{\partial x^2} \\[4mm] N_{xy_{jm}} = -\dfrac{\partial^2 \phi_{jm}}{\partial x\, \partial y} \end{array}\right\} \tag{B2}$$

$$(j = 1,\ 2)$$

and

$$\nabla^4 \phi_{jm} = 0 \qquad (j = 1,\ 2) \tag{B3}$$

These force functions satisfy the equations of equilibrium in each bay (eqs. (A1)) and ensure the compatibility of the strains derived from the middle-surface forces. Suitable stress functions for the present problem are

$$\phi_{jm} = \left[\left(A_{jm} + \frac{m\pi y}{a} B_{jm}\right)\sinh \frac{m\pi y}{a} + \left(C_{jm} + \frac{m\pi y}{a} D_{jm}\right)\cosh \frac{m\pi y}{a}\right]\sin \frac{m\pi x}{a} \quad (B4)$$

From equations (B2) and the stress-strain relations given by equations (A2) and (A3), the following expressions for the forces and displacements in each bay can be obtained:

For the forces,

$$N_{x_{jm}} = \left[\left(A_{jm} + 2D_{jm} + \frac{m\pi y}{a} B_{jm}\right)\sinh \frac{m\pi y}{a} + \right.$$

$$\left. \left(C_{jm} + 2B_{jm} + \frac{m\pi y}{a} D_{jm}\right)\cosh \frac{m\pi y}{a}\right]\left(\frac{m\pi}{a}\right)^2 \sin \frac{m\pi x}{a} \quad (B5a)$$

$$N_{y_{jm}} = -\left[\left(A_{jm} + \frac{m\pi y}{a} B_{jm}\right)\sinh \frac{m\pi y}{a} + \right.$$

$$\left. \left(C_{jm} + \frac{m\pi y}{a} D_{jm}\right)\cosh \frac{m\pi y}{a}\right]\left(\frac{m\pi}{a}\right)^2 \sin \frac{m\pi x}{a} \quad (B5b)$$

$$N_{xy_{jm}} = -\left[\left(A_{jm} + D_{jm} + \frac{m\pi y}{a} B_{jm}\right)\cosh \frac{m\pi y}{a} + \right.$$

$$\left. \left(C_{jm} + B_{jm} + \frac{m\pi y}{a} D_{jm}\right)\sinh \frac{m\pi y}{a}\right]\left(\frac{m\pi}{a}\right)^2 \cos \frac{m\pi x}{a} \quad (B5c)$$

and, for the displacements,

$$Etu_{jm} = -\left\{\left[(1 + \mu)\left(A_{jm} + \frac{m\pi y}{a} B_{jm}\right) + 2D_{jm}\right]\sinh \frac{m\pi y}{a} + \right.$$

$$\left.\left[(1 + \mu)\left(C_{jm} + \frac{m\pi y}{a} D_{jm}\right) + 2B_{jm}\right]\cosh \frac{m\pi y}{a}\right\}\frac{m\pi}{a} \cos \frac{m\pi x}{a} \qquad (B6a)$$

$$Etv_{jm} = -\left\{\left[(1 + \mu)\left(A_{jm} + \frac{m\pi y}{a} B_{jm}\right) - (1 - \mu)D_{jm}\right]\cosh \frac{m\pi y}{a} + \right.$$

$$\left.\left[(1 + \mu)\left(C_{jm} + \frac{m\pi y}{a} D_{jm}\right) - (1 - \mu)B_{jm}\right]\sinh \frac{m\pi y}{a}\right\}\frac{m\pi}{a} \sin \frac{m\pi x}{a}$$

$$(B6b)$$

Rigid body displacements are left out of the expressions for u_{jm} and v_{jm} since they do not influence the solution of the elasticity problem.

It is seen that the forces and displacements already satisfy some of the boundary conditions that are imposed. The displacements in the y-direction and the normal forces vanish at the edges ($x = 0$ and $x = a$). The conditions at the line of application $\left(y = k\frac{b}{2}\right)$ of the shear force (eqs. (A5)) yield the following conditions that must be satisfied by the unknown coefficients of the stress functions:

$$\left(A_{2m} - A_{1m}\right)\cosh \frac{km\pi b}{2a} + \left(B_{2m} - B_{1m}\right)\left(\frac{km\pi b}{2a} \cosh \frac{km\pi b}{2a} + \sinh \frac{km\pi b}{2a}\right) +$$

$$\left(C_{2m} - C_{1m}\right)\sinh \frac{km\pi b}{2a} + \left(D_{2m} - D_{1m}\right)\left(\frac{km\pi b}{2a} \sinh \frac{km\pi b}{2a} + \cosh \frac{km\pi b}{2a}\right) = \left(\frac{a}{m\pi}\right)^2 F_m$$

$$(B7a)$$

$$\left(A_{2m} - A_{1m}\right)\sinh\frac{km\pi b}{2a} + \left(B_{2m} - B_{1m}\right)\frac{km\pi b}{2a}\sinh\frac{km\pi b}{2a} +$$

$$\left(C_{2m} - C_{1m}\right)\cosh\frac{km\pi b}{2a} + \left(D_{2m} - D_{1m}\right)\frac{km\pi b}{2a}\cosh\frac{km\pi b}{2a} = 0 \qquad \text{(B7b)}$$

$$\left(A_{2m} - A_{1m}\right)\sinh\frac{km\pi b}{2a} + \left(B_{2m} - B_{1m}\right)\left(\frac{km\pi b}{2a}\sinh\frac{km\pi b}{2a} + \frac{2}{1+\mu}\cosh\frac{km\pi b}{2a}\right) +$$

$$\left(C_{2m} - C_{1m}\right)\cosh\frac{km\pi b}{2a} + \left(D_{2m} - D_{1m}\right)\left(\frac{km\pi b}{2a}\cosh\frac{km\pi b}{2a} + \frac{2}{1+\mu}\sinh\frac{km\pi b}{2a}\right) = 0$$

$$\text{(B7c)}$$

$$\left(A_{2m} - A_{1m}\right)\cosh\frac{km\pi b}{2a} + \left(B_{2m} - B_{1m}\right)\left(\frac{km\pi b}{2a}\cosh\frac{km\pi b}{2a} - \frac{1-\mu}{1+\mu}\sinh\frac{km\pi b}{2a}\right) +$$

$$\left(C_{2m} - C_{1m}\right)\sinh\frac{km\pi b}{2a} + \left(D_{2m} - D_{1m}\right)\left(\frac{km\pi b}{2a}\sinh\frac{km\pi b}{2a} - \frac{1-\mu}{1+\mu}\cosh\frac{km\pi b}{2a}\right) = 0$$

$$\text{(B7d)}$$

From equations (B7) the following equations can be obtained:

$$A_{2m} - A_{1m} = \frac{1+\mu}{2}\left(\frac{1-\mu}{1+\mu}\cosh\frac{km\pi b}{2a} + \frac{km\pi b}{2a}\sinh\frac{km\pi b}{2a}\right)\left(\frac{a}{m\pi}\right)^2 F_m \qquad \text{(B8a)}$$

$$B_{2m} - B_{1m} = -\frac{1+\mu}{2}\sinh\frac{km\pi b}{2a}\left(\frac{a}{m\pi}\right)^2 F_m \qquad \text{(B8b)}$$

$$C_{2m} - C_{1m} = -\frac{1+\mu}{2}\left(\frac{1-\mu}{1+\mu}\sinh\frac{km\pi b}{2a} + \frac{km\pi b}{2a}\cosh\frac{km\pi b}{2a}\right)\left(\frac{a}{m\pi}\right)^2 F_m \qquad \text{(B8c)}$$

$$D_{2m} - D_{1m} = \frac{1+\mu}{2}\cosh\frac{km\pi b}{2a}\left(\frac{a}{m\pi}\right)^2 F_m \qquad \text{(B8d)}$$

Four more equations from which the coefficients of the force functions can be determined are obtained from the conditions at the edges $y = \pm\dfrac{b}{2}$ of the plate; that is, the middle-surface forces normal and tangential to these edges vanish. Then

$$A_{2m} \sinh \frac{m\pi b}{2a} + B_{2m} \frac{m\pi b}{2a} \sinh \frac{m\pi b}{2a} + C_{2m} \cosh \frac{m\pi b}{2a} + D_{2m} \frac{m\pi b}{2a} \cosh \frac{m\pi b}{2a} = 0$$

$$\text{(B9a)}$$

$$A_{2m} \cosh \frac{m\pi b}{2a} + B_{2m}\left(\frac{m\pi b}{2a} \cosh \frac{m\pi b}{2a} + \sinh \frac{m\pi b}{2a}\right) +$$

$$C_{2m} \sinh \frac{m\pi b}{2a} + D_{2m}\left(\frac{m\pi b}{2a} \sinh \frac{m\pi b}{2a} + \cosh \frac{m\pi b}{2a}\right) = 0 \qquad \text{(B9b)}$$

$$A_{1m} \sinh \frac{m\pi b}{2a} - B_{1m} \frac{m\pi b}{2a} \sinh \frac{m\pi b}{2a} - C_{1m} \cosh \frac{m\pi b}{2a} + D_{1m} \frac{m\pi b}{2a} \cosh \frac{m\pi b}{2a} = 0$$

$$\text{(B9c)}$$

$$A_{1m} \cosh \frac{m\pi b}{2a} - B_{1m}\left(\frac{m\pi b}{2a} \cosh \frac{m\pi b}{2a} + \sinh \frac{m\pi b}{2a}\right) -$$

$$C_{1m} \sinh \frac{m\pi b}{2a} + D_{1m}\left(\frac{m\pi b}{2a} \sinh \frac{m\pi b}{2a} + \cosh \frac{m\pi b}{2a}\right) = 0 \qquad \text{(B9d)}$$

from which are obtained

$$A_{2m} + A_{1m} = \frac{1+\mu}{4}\left(\frac{a}{m\pi}\right)^2 F_m \frac{\left\{ \begin{array}{l} -4\left(\dfrac{m\pi b}{2a}\right)^2 \sinh \dfrac{km\pi b}{2a} + \\[2mm] \dfrac{km\pi b}{2a}\left[\cosh(2+k)\dfrac{m\pi b}{2a} + \cosh(2-k)\dfrac{m\pi b}{2a} + 2\cosh\dfrac{km\pi b}{2a}\right] + \\[2mm] \dfrac{1-\mu}{1+\mu}\left[\sinh(2+k)\dfrac{m\pi b}{2a} - \sinh(2-k)\dfrac{m\pi b}{2a} + 2\sinh\dfrac{km\pi b}{2a}\right] \end{array} \right\}}{\sinh\dfrac{m\pi b}{a} - \dfrac{m\pi b}{a}} \qquad \text{(B10a)}$$

$$
B_{2m} + B_{1m} = -\frac{1+\mu}{4}\left(\frac{a}{m\pi}\right)^2 F_m \frac{\left\{\begin{array}{l} \cosh(2+k)\dfrac{m\pi b}{2a} + \cosh(2-k)\dfrac{m\pi b}{2a} + \\[2mm] 2\dfrac{3-\mu}{1+\mu}\cosh\dfrac{km\pi b}{2a} + \dfrac{4km\pi b}{2a}\sinh\dfrac{km\pi b}{2a} \end{array}\right\}}{\sinh\dfrac{m\pi b}{a} + \dfrac{m\pi b}{a}}
$$

$$\text{(B10b)}$$

$$
C_{2m} + C_{1m} = -\frac{1+\mu}{4}\left(\frac{a}{m\pi}\right)^2 F_m \frac{\left\{\begin{array}{l} \dfrac{1-\mu}{1+\mu}\left[\cosh(2+k)\dfrac{m\pi b}{2a} + \cosh(2-k)\dfrac{m\pi b}{2a} - \right.\\[2mm] \left. 2\cosh\dfrac{km\pi b}{2a}\right] + \dfrac{km\pi b}{2a}\left[\sinh(2+k)\dfrac{m\pi b}{2a} - \right.\\[2mm] \left. \sinh(2-k)\dfrac{m\pi b}{2a} - 2\sinh\dfrac{km\pi b}{2a}\right] \cdot\\[2mm] 4\left(\dfrac{m\pi b}{2a}\right)^2\cosh\dfrac{km\pi b}{2a} \end{array}\right\}}{\sinh\dfrac{m\pi b}{a} + \dfrac{m\pi b}{a}}
$$

$$\text{(B10c)}$$

$$
D_{2m} + D_{1m} = \frac{1+\mu}{4}\left(\frac{a}{m\pi}\right)^2 F_m \frac{\left\{\begin{array}{l} \sinh(2+k)\dfrac{m\pi b}{2a} - \sinh(2-k)\dfrac{m\pi b}{2a} - \\[2mm] 2\dfrac{3-\mu}{1+\mu}\sinh\dfrac{km\pi b}{2a} - \dfrac{4km\pi b}{2a}\cosh\dfrac{km\pi b}{2a} \end{array}\right\}}{\sinh\dfrac{m\pi b}{a} - \dfrac{m\pi b}{a}}
$$

$$\text{(B10d)}$$

Solution of equations (B8) and (B10) then yields

$$
A_{1m} = \frac{1+\mu}{4}\left(\frac{a}{m\pi}\right)^2 F_m \cdot \frac{\left\{ \left(2\,\dfrac{1-\mu}{1+\mu}+k\right)\dfrac{m\pi b}{2a}\cosh\dfrac{km\pi b}{2a} - \left[2(1-k)\left(\dfrac{m\pi b}{2a}\right)^2 - \dfrac{1-\mu}{1+\mu}\right]\sinh\dfrac{km\pi b}{2a} + \dfrac{km\pi b}{2a}\cosh(2-k)\dfrac{m\pi b}{2a} - \dfrac{1-\mu}{1+\mu}\sinh(2-k)\dfrac{m\pi b}{2a} \right\}}{\sinh\dfrac{m\pi b}{a} - \dfrac{m\pi b}{a}}
$$

(B11a)

$$
B_{1m} = -\frac{1+\mu}{4}\left(\frac{a}{m\pi}\right)^2 F_m \frac{\left\{ \dfrac{3-\mu}{1+\mu}\cosh\dfrac{km\pi b}{2a} - 2(1-k)\dfrac{m\pi b}{2a}\sinh\dfrac{km\pi b}{2a} + \cosh(2-k)\dfrac{m\pi b}{2a} \right\}}{\sinh\dfrac{m\pi b}{a} + \dfrac{m\pi b}{a}}
$$

(B11b)

$$
C_{1m} = -\frac{1+\mu}{4}\left(\frac{a}{m\pi}\right)^2 F_m \frac{\left\{ \left[2(1-k)\left(\dfrac{m\pi b}{2a}\right)^2 - \dfrac{1-\mu}{1+\mu}\right]\cosh\dfrac{km\pi b}{2a} - \left(2\,\dfrac{1-\mu}{1+\mu}+k\right)\dfrac{m\pi b}{2a}\sinh\dfrac{km\pi b}{2a} + \dfrac{1-\mu}{1+\mu}\cosh(2-k)\dfrac{m\pi b}{2a} - \dfrac{km\pi b}{2a}\sinh(2-k)\dfrac{m\pi b}{2a} \right\}}{\sinh\dfrac{m\pi b}{a} + \dfrac{m\pi b}{a}}
$$

(B11c)

$$D_{1m} = \frac{1 + \mu}{4}\left(\frac{a}{m\pi}\right)^2 F_m \frac{\left\{\begin{array}{l} 2(1 - k)\dfrac{m\pi b}{2a}\cosh\dfrac{km\pi b}{2a} - \\[2mm] \dfrac{3 - \mu}{1 + \mu}\sinh\dfrac{km\pi b}{2a} - \sinh(2 - k)\dfrac{m\pi b}{2a} \end{array}\right\}}{\sinh\dfrac{m\pi b}{a} - \dfrac{m\pi b}{a}} \qquad \text{(B11d)}$$

and

$$A_{2m} = \frac{1 + \mu}{4}\left(\frac{a}{m\pi}\right)^2 F_m \frac{\left\{\begin{array}{l}\left(k - 2\dfrac{1 - \mu}{1 + \mu}\right)\dfrac{m\pi b}{2a}\cosh\dfrac{km\pi b}{2a} - \left[2(1 + k)\left(\dfrac{m\pi b}{2a}\right)^2 - \right. \\[2mm] \left. \dfrac{1 - \mu}{1 + \mu}\right]\sinh\dfrac{km\pi b}{2a} + \dfrac{km\pi b}{2a}\cosh(2 + k)\dfrac{m\pi b}{2a} + \\[2mm] \dfrac{1 - \mu}{1 + \mu}\sinh(2 + k)\dfrac{m\pi b}{2a} \end{array}\right\}}{\sinh\dfrac{m\pi b}{a} - \dfrac{m\pi b}{a}}$$

$$\text{(B12a)}$$

$$B_{2m} = -\frac{1 + \mu}{4}\left(\frac{a}{m\pi}\right)^2 F_m \frac{\left\{\begin{array}{l}\dfrac{3 - \mu}{1 + \mu}\cosh\dfrac{km\pi b}{2a} + 2(1 + k)\dfrac{m\pi b}{2a}\sinh\dfrac{km\pi b}{2a} + \\[2mm] \cosh(2 + k)\dfrac{m\pi b}{2a} \end{array}\right\}}{\sinh\dfrac{m\pi b}{a} + \dfrac{m\pi b}{a}}$$

$$\text{(B12b)}$$

$$C_{2m} = -\frac{1 + \mu}{4}\left(\frac{a}{m\pi}\right)^2 F_m \frac{\left\{\begin{array}{l}\left[2(1 + k)\left(\dfrac{m\pi b}{2a}\right)^2 - \dfrac{1 - \mu}{1 + \mu}\right]\cosh\dfrac{km\pi b}{2a} + \\[2mm] \dfrac{1 - \mu}{1 + \mu}\cosh(2 + k)\dfrac{m\pi b}{2a} + \left(2\dfrac{1 - \mu}{1 + \mu} - \right. \\[2mm] \left. k\right)\dfrac{m\pi b}{2a}\sinh\dfrac{km\pi b}{2a} + \dfrac{km\pi b}{2a}\sinh(2 + k)\dfrac{m\pi b}{2a} \end{array}\right\}}{\sinh\dfrac{m\pi b}{a} + \dfrac{m\pi b}{a}} \qquad \text{(B12c)}$$

$$D_{2m} = \frac{1+\mu}{4}\left(\frac{a}{m\pi}\right)^2 F_m \frac{\sinh(2+k)\frac{m\pi b}{2a} - 2(1+k)\cosh\frac{km\pi b}{2a} - \frac{3-\mu}{1+\mu}\sinh\frac{km\pi b}{2a}}{\sinh\frac{m\pi b}{a} - \frac{m\pi b}{a}} \tag{B12d}$$

Of particular interest are the displacements in the x-direction of the plate middle surface. These displacements are determined for bay 1 by substituting equations (B11) into equation (B6a) to obtain

$$
\begin{aligned}
u_{1m} = \Bigg(& \frac{1}{\sinh\frac{m\pi b}{a} + \frac{m\pi b}{a}}\Bigg\{(3-\mu)(1+\mu)\left[\cosh\left(2+\frac{2y}{b}-k\right)\frac{m\pi b}{2a} + \cosh\left(2-\frac{2y}{b}-k\right)\frac{m\pi b}{2a}\right] + \\
& \left[5-2\mu+\mu^2+2(1+\mu)^2(1-k)\left(1-\frac{2y}{b}\right)\left(\frac{m\pi b}{2a}\right)^2\right]\cosh\left(\frac{2y}{b}+k\right)\frac{m\pi b}{2a} + \\
& \left[5-2\mu+\mu^2+2(1+\mu)^2(1-k)\left(1+\frac{2y}{b}\right)\left(\frac{m\pi b}{2a}\right)^2\right]\cosh\left(\frac{2y}{b}-k\right)\frac{m\pi b}{2a} + \\
& (1+\mu)^2\frac{m\pi b}{2a}\left[\left(\frac{2y}{b}-k\right)\sinh\left(2+\frac{2y}{b}-k\right)\frac{m\pi b}{2a} - \left(\frac{2y}{b}+k\right)\sinh\left(2-\frac{2y}{b}-k\right)\frac{m\pi b}{2a}\right] - \\
& (3-\mu)(1+\mu)\frac{m\pi b}{2a}\left[\left(2-\frac{2y}{b}-k\right)\sinh\left(\frac{2y}{b}+k\right)\frac{m\pi b}{2a} - \left(2+\frac{2y}{b}-k\right)\sinh\left(\frac{2y}{b}-k\right)\frac{m\pi b}{2a}\right]\Bigg\} + \\
& \frac{1}{\sinh\frac{m\pi b}{a} - \frac{m\pi b}{a}}\Bigg\{(3-\mu)(1+\mu)\left[\cosh\left(2+\frac{2y}{b}-k\right)\frac{m\pi b}{2a} - \cosh\left(2-\frac{2y}{b}-k\right)\frac{m\pi b}{2a}\right] + \\
& \left[5-2\mu+\mu^2+2(1+\mu)^2(1-k)\left(1-\frac{2y}{b}\right)\left(\frac{m\pi b}{2a}\right)^2\right]\cosh\left(\frac{2y}{b}+k\right)\frac{m\pi b}{2a} - \\
& \left[5-2\mu+\mu^2+2(1+\mu)^2(1-k)\left(1+\frac{2y}{b}\right)\left(\frac{m\pi b}{2a}\right)^2\right]\cosh\left(\frac{2y}{b}-k\right)\frac{m\pi b}{2a} + \\
& (1+\mu)^2\frac{m\pi b}{2a}\left[\left(\frac{2y}{b}-k\right)\sinh\left(2+\frac{2y}{b}-k\right)\frac{m\pi b}{2a} + \left(\frac{2y}{b}+k\right)\sinh\left(2-\frac{2y}{b}-k\right)\frac{m\pi b}{2a}\right] - \\
& (3-\mu)(1+\mu)\frac{m\pi b}{2a}\left[\left(2-\frac{2y}{b}-k\right)\sinh\left(\frac{2y}{b}+k\right)\frac{m\pi b}{2a} + \right. \\
& \left. \left(2+\frac{2y}{b}-k\right)\sinh\left(\frac{2y}{b}-k\right)\frac{m\pi b}{2a}\right]\Bigg\}\Bigg)\frac{1}{8}\frac{a}{m\pi}\frac{F_m}{Et}\cos\frac{m\pi x}{a} \tag{B13}
\end{aligned}
$$

and for bay 2 by substituting equations (B12) into equation (B6a) to obtain

$$
\begin{aligned}
u_{2m} = \Bigg(& \frac{1}{\sinh\frac{m\pi b}{a} + \frac{m\pi b}{a}} \Bigg\{ (3-\mu)(1+\mu)\left[\cosh\left(2+\frac{2y}{b}+k\right)\frac{m\pi b}{2a} + \cosh\left(2-\frac{2y}{b}+k\right)\frac{m\pi b}{2a}\right] + \\
& \left[5 - 2\mu + \mu^2 + 2(1+\mu)^2(1+k)\left(1+\frac{2y}{b}\right)\left(\frac{m\pi b}{2a}\right)^2\right]\cosh\left(\frac{2y}{b}+k\right)\frac{m\pi b}{2a} + \\
& \left[5 - 2\mu + \mu^2 + 2(1+\mu)^2(1+k)\left(1-\frac{2y}{b}\right)\left(\frac{m\pi b}{2a}\right)^2\right]\cosh\left(\frac{2y}{b}-k\right)\frac{m\pi b}{2a} + \\
& (1+\mu)^2\frac{m\pi b}{2a}\left[\left(\frac{2y}{b}+k\right)\sinh\left(2+\frac{2y}{b}+k\right)\frac{m\pi b}{2a} - \left(\frac{2y}{b}-k\right)\sinh\left(2-\frac{2y}{b}+k\right)\frac{m\pi b}{2a}\right] + \\
& (3-\mu)(1+\mu)\frac{m\pi b}{2a}\left[\left(2+\frac{2y}{b}+k\right)\sinh\left(\frac{2y}{b}+k\right)\frac{m\pi b}{2a} - \left(2-\frac{2y}{b}+k\right)\sinh\left(\frac{2y}{b}-k\right)\frac{m\pi b}{2a}\right]\Bigg\} - \\
& \frac{1}{\sinh\frac{m\pi b}{a} - \frac{m\pi b}{a}} \Bigg\{ (3-\mu)(1+\mu)\left[\cosh\left(2+\frac{2y}{b}+k\right)\frac{m\pi b}{2a} - \cosh\left(2-\frac{2y}{b}+k\right)\frac{m\pi b}{2a}\right] - \\
& \left[5 - 2\mu + \mu^2 + 2(1+\mu)^2(1+k)\left(1+\frac{2y}{b}\right)\left(\frac{m\pi b}{2a}\right)^2\right]\cosh\left(\frac{2y}{b}+k\right)\frac{m\pi b}{2a} + \\
& \left[5 - 2\mu + \mu^2 + 2(1+\mu)^2(1+k)\left(1-\frac{2y}{b}\right)\left(\frac{m\pi b}{2a}\right)^2\right]\cosh\left(\frac{2y}{b}-k\right)\frac{m\pi b}{2a} + \\
& (1+\mu)^2\frac{m\pi b}{2a}\left[\left(\frac{2y}{b}+k\right)\sinh\left(2+\frac{2y}{b}+k\right)\frac{m\pi b}{2a} + \left(\frac{2y}{b}-k\right)\sinh\left(2-\frac{2y}{b}+k\right)\frac{m\pi b}{2a}\right] - \\
& (3-\mu)(1+\mu)\frac{m\pi b}{2a}\left[\left(2+\frac{2y}{b}+k\right)\sinh\left(\frac{2y}{b}+k\right)\frac{m\pi b}{2a} + \\
& \left(2-\frac{2y}{b}+k\right)\sinh\left(\frac{2y}{b}-k\right)\frac{m\pi b}{2a}\right]\Bigg\} \Bigg) \frac{1}{8}\frac{a}{m\pi}\frac{F_m}{Et}\cos\frac{m\pi x}{a}
\end{aligned}
$$

(B14)

Plate With Infinitely Many Stiffeners

For the assumed buckling configuration of a plate with infinitely many stiffeners, a separate derivation of the middle-surface forces and displacements must be made. It is apparent from considerations of symmetry that only one-half of a bay of the plate need be considered and that the conditions that must be satisfied at the edges of this half-bay are given by

$$
\left.
\begin{aligned}
N_{xy}' &= v' = 0 && \text{at} \quad y = \frac{d}{2} \\[2mm]
N_{xy}' &= \frac{F_\infty}{2} && \text{at} \quad y = 0 \\[2mm]
v' &= 0 && \text{at} \quad y = 0
\end{aligned}
\right\}
\qquad (B15)
$$

The shear force F_∞ may be expressed as

$$
F_\infty = F_m' \cos \frac{m\pi x}{a} \tag{B16}
$$

and the appropriate force function for the half-bay is given by

$$
\phi_m' = \left[\left(A_m' + \frac{m\pi y}{a} B_m' \right) \sinh \frac{m\pi y}{a} + \left(C_m' + \frac{m\pi y}{a} D_m' \right) \cosh \frac{m\pi y}{a} \right] \sin \frac{m\pi x}{a} \tag{B17}
$$

which is similar to equation (B4). Expressions similar to equations (B5) and (B6) are obtained for middle-surface forces and displacements in the plate. The substitution of these expressions into equations (B15) yields

$$
(1 + \mu) A_m' - (1 - \mu) D_m' = 0 \tag{B18a}
$$

$$
A_m' + D_m' = \left(\frac{a}{m\pi} \right)^2 \frac{F_m'}{2} \tag{B18b}
$$

$$A_m' \cosh \frac{m\pi d}{2a} + B_m'\left(\frac{m\pi d}{2a} \cosh \frac{m\pi d}{2a} - \frac{1-\mu}{1+\mu} \sinh \frac{m\pi d}{2a}\right) +$$

$$C_m' \sinh \frac{m\pi d}{2a} + D_m'\left(\frac{m\pi d}{2a} \sinh \frac{m\pi d}{2a} - \frac{1-\mu}{1+\mu} \cosh \frac{m\pi d}{2a}\right) = 0 \qquad \text{(B18c)}$$

$$A_m' \cosh \frac{m\pi d}{2a} + B_m'\left(\frac{m\pi d}{2a} \cosh \frac{m\pi d}{2a} + \sinh \frac{m\pi d}{2a}\right) +$$

$$C_m' \sinh \frac{m\pi d}{2a} + D_m'\left(\frac{m\pi d}{2a} \sinh \frac{m\pi d}{2a} + \cosh \frac{m\pi d}{2a}\right) = 0 \qquad \text{(B18d)}$$

The solution of these equations for A_m', B_m', C_m', and D_m' yields

$$A_m' = \frac{1-\mu}{4}\left(\frac{a}{m\pi}\right)^2 F_m' \qquad \text{(B19a)}$$

$$B_m' = -\frac{1+\mu}{4} \coth \frac{m\pi d}{2a}\left(\frac{a}{m\pi}\right)^2 F_m' \qquad \text{(B19b)}$$

$$C_m' = -\frac{1+\mu}{4} \frac{\dfrac{1-\mu}{1+\mu} \sinh \dfrac{m\pi d}{a} - \dfrac{m\pi d}{a}}{\cosh \dfrac{m\pi d}{a} - 1}\left(\frac{a}{m\pi}\right)^2 F_m' \qquad \text{(B19c)}$$

$$D_m' = \frac{1+\mu}{4}\left(\frac{a}{m\pi}\right)^2 F_m' \qquad \text{(B19d)}$$

The displacements along the line of application of the force, which are of particular interest, are then given by

$$\left(u_m'\right)_{y=0} = \frac{1+\mu}{4} \frac{(3-\mu)\sinh \dfrac{m\pi d}{a} - (1+\mu)\dfrac{m\pi d}{a}}{\cosh \dfrac{m\pi d}{a} - 1} \frac{a}{m\pi} \frac{F_m'}{Et} \cos \frac{m\pi x}{a} \qquad \text{(B20)}$$

Forces and Displacements in the Stiffeners

To each stiffener, forces per unit length of the form

$$F_i = F_{im} \cos \frac{m\pi x}{a} \qquad (i = 1, 2, \ldots (N-1)) \qquad (B21)$$

are applied. From equations (A6), the force in the stiffener is related to the applied shear force by

$$\frac{dP_i}{dx} = F_{im} \cos \frac{m\pi x}{a} \qquad (i = 1, 2, \ldots (N-1)) \qquad (B22)$$

in which case

$$P_i = \frac{a}{m\pi} F_{im} \sin \frac{m\pi x}{a} \qquad (i = 1, 2, \ldots (N-1)) \qquad (B23)$$

Constants of integration vanish since each load P_i must vanish at the ends of the stiffeners. Displacements in the stiffeners are then obtained from the forces by the use of equations (A8) and (A9), which yield

$$u_{S_i} = -\left(\frac{a}{m\pi}\right)^2 \frac{F_{im}}{EA_S} \cos \frac{m\pi x}{a} \qquad (i = 1, 2, \ldots (N-1)) \qquad (B24)$$

Constants of integration are omitted since they represent rigid body motions and have no effect on the problem.

REFERENCES

1. Timoshenko, S.: On the Stability of Stiffened Plates. Rep. No. 402,
   U. S. Exp. Model Basin, Washington Navy Yard, 1935. (From Der
   Eisenbau, vol. 12, 1921, pp. 147-163.)

2. Timoshenko, S., and Goodier, J. N.: Theory of Elasticity. Second
   ed., McGraw-Hill Book Co., Inc., 1951, pp. 171-177.

3. Smith, C. B., Heebink, T. B., and Norris, C. B.: The Effective
   Stiffness of a Stiffener Attached to a Flat Plywood Plate. Rep.
   No. 1557, Forest Products Lab., U. S. Dept. Agric., Sept. 1946.

4. Odqvist, Folke: On the Effective Width of Reinforced Plane Plates.
   Translation No. 5, Royal Swedish Air Board (Stockholm), 1948.

5. Chwalla, E., and Novak, A.: The Theory of One-Sided Web Stiffeners.
   R.T.P. 3 Translation No. 2501, British M.A.P. (Bautechnik (Supple-
   ment der Stahlbau), vol. 10, no. 10, May 7, 1937, pp. 73-76.)

6. Cox, H. L., and Riddell, J. R.: Buckling of a Longitudinally
   Stiffened Flat Panel. Rep. No. 11,374, British A.R.C., Apr. 3,
   1948.

7. Freyer, R.: Zur Stabilität einer anisotropen Platte. Tech.
   Berichte der Z.W.B., Bd. 11, Heft 7, July 15, 1944, pp. 231-234.

8. Pfluger, A.: The Buckling of Anisotropic Rectangular Plates (Sheets).
   Rep. No. 1537, McDonnell Aircraft Corp., Oct. 1949. (Zum Beulproblem
   der anistropen Rechteckplatte. Ing.-Archiv, Bd. XVI, 1947.)

9. Seide, Paul, and Stein, Manuel: Compressive Buckling of Simply
   Supported Plates With Longitudinal Stiffeners. NACA TN 1825, 1949.

10. Timoshenko, S.: Theory of Elastic Stability. McGraw-Hill Book Co.,
    Inc., 1936.

11. Budiansky, Bernard, Seide, Paul, and Weinberger, Robert A.: The
    Buckling of a Column on Equally Spaced Deflectional and Rotational
    Springs. NACA TN 1519, 1948.

TABLE I

VARIATION OF Z_{Nq} WITH BUCKLE ASPÉCT RATIO

$$\left[\mu = \frac{1}{3}\right]$$

$\dfrac{a/d}{m}$	Z_{Nq}				
	N = 2	N = 3		N = 4	N = ∞
	q = 1	q = 1	q = 2	q = 2	$\dfrac{q}{N} = 0$
∞	0.500	0.667	0.222	0.375	0.889
31.416	.505	.672	.228	.381	.892
15.706	.520	.689	.247	.401	.898
10.472	.545	.716	.276	.437	.909
7.854	.579	.755	.318	.471	.924
6.283	.622	.799	.370	.532	.944
5.236	.673	.853	.432	.596	.968
4.488	.733	.913	.502	.668	.996
3.927	.799	.973	.574	.748	1.029
3.491	.872	1.047	.667	.832	1.065
3.142	.950	1.119	.759	.921	1.105
2.513	1.162	1.303	1.007	1.153	1.222
2.094	1.390	1.486	1.269	1.389	1.360
1.795	1.621	1.668	1.535	1.620	1.517
1.571	1.850	1.851	1.796	1.845	1.691
1.257	2.293	2.231	2.292	2.278	2.078
1.047	2.721	2.636	2.755	2.708	2.505
.785	3.578	3.498	3.631	3.570	3.418
.628	4.451	4.403	4.493	4.449	4.353
.524	5.335	5.308	5.320	5.334	5.280
.393	7.111	7.104	7.118	7.111	7.097
.314	8.889	8.889	8.889	8.889	8.886
.209	13.333	13.333	13.333	13.333	13.333
.157	17.778	17.778	17.778	17.778	17.778
.000	∞	∞	∞	∞	∞

NACA

TABLE II

VARIATION WITH BUCKLE ASPECT RATIO OF η FUNCTIONS FOR

BUCKLING SYMMETRICAL ABOUT THE LONGITUDINAL CENTER

LINE OF A PLATE WITH THREE STIFFENERS

| $\frac{a/d}{m}$	η_1	η_2	η_3	η_4	η_5	η_6
∞	0.021	0.500	0.250	0.354	0.729	0.125
31.416	.031	.519	.260	.353	.737	.129
15.706	.079	.572	.289	.351	.782	.141
10.472	.149	.657	.337	.348	.845	.160
7.854	.242	.770	.400	.343	.928	.185
6.283	.351	.899	.475	.336	1.023	.212
5.236	.472	1.039	.559	.327	1.1£	.240
4.488	.600	1.181	.651	.316	1.23_	.265
3.927	.729	1.317	.742	.301	1.331	.287
3.491	.854	1.442	.834	.283	1.421	.304
3.142	.976	1.553	.925	.263	1.502	.314
2.513	1.238	1.771	1.112	.203	1.644	.329
2.094	1.505	1.926	1.361	.138	1.782	.283
1.795	1.739	2.055	1.574	.076	1.890	.241
1.571	1.903	2.181	1.789	.022	2.007	.196
1.257	2.396	2.461	2.223	-.053	2.289	.119
1.047	2.876	2.806	2.668	-.089	2.698	.069
.785	3.665	3.592	3.556	-.091	3.481	.018
.628	4.514	4.458	4.444	-.063	4.388	.006
.524	5.372	5.335	5.333	-.037	5.297	.001
.393	7.121	7.111	7.111	-.010	7.101	.000
.314	8.891	8.889	8.889	.000	8.887	.000
.209	13.333	13.333	13.333	.000	13.333	.000
.157	17.778	17.778	17.778	.000	17.778	.000
.000	∞	∞	∞	.000	∞	.000
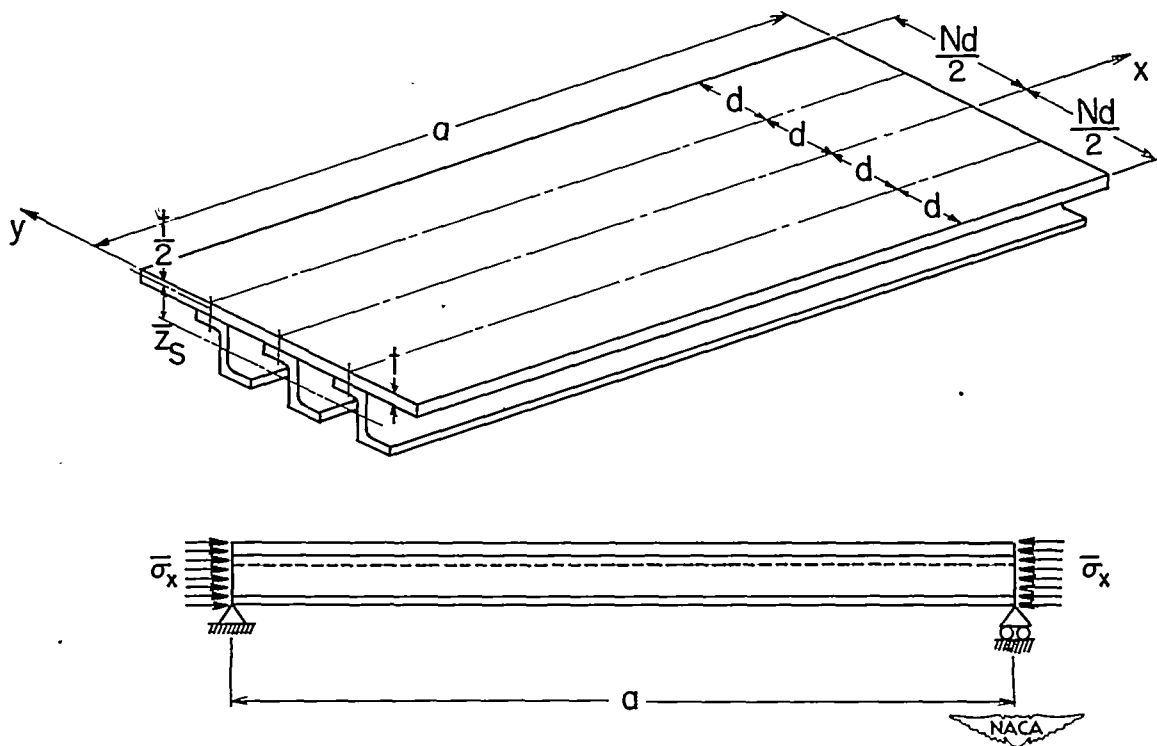
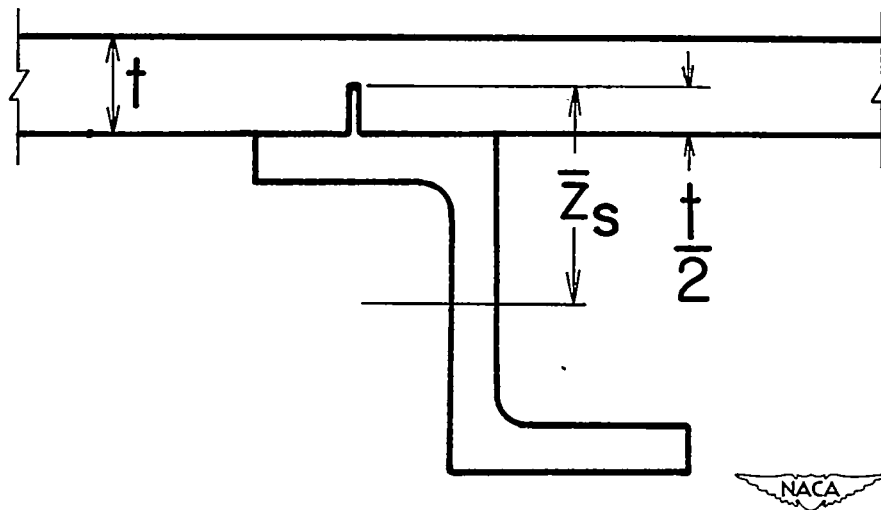Figure 1.- Compressed plate with equal and equally spaced longitudinal
stiffeners on one side.

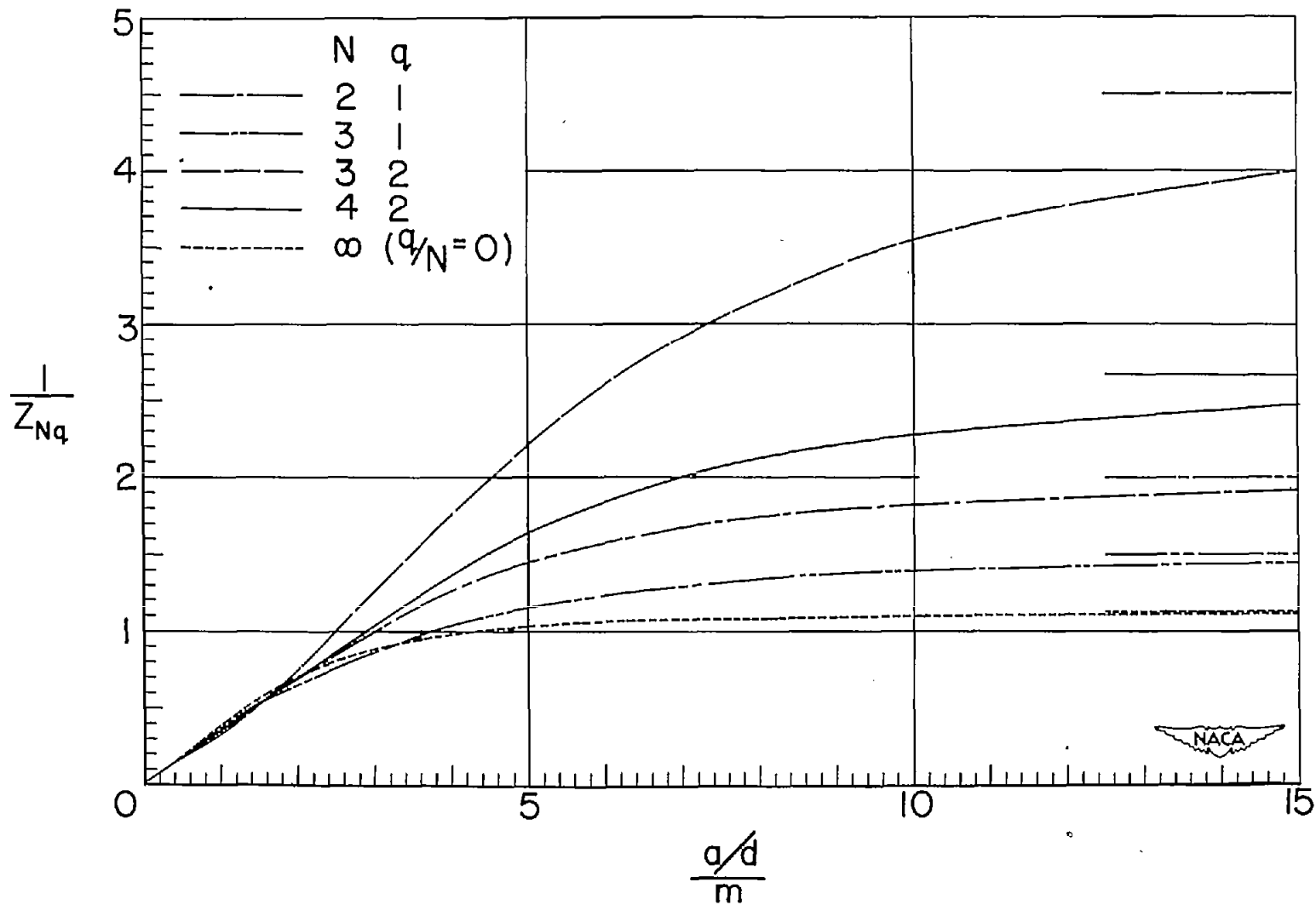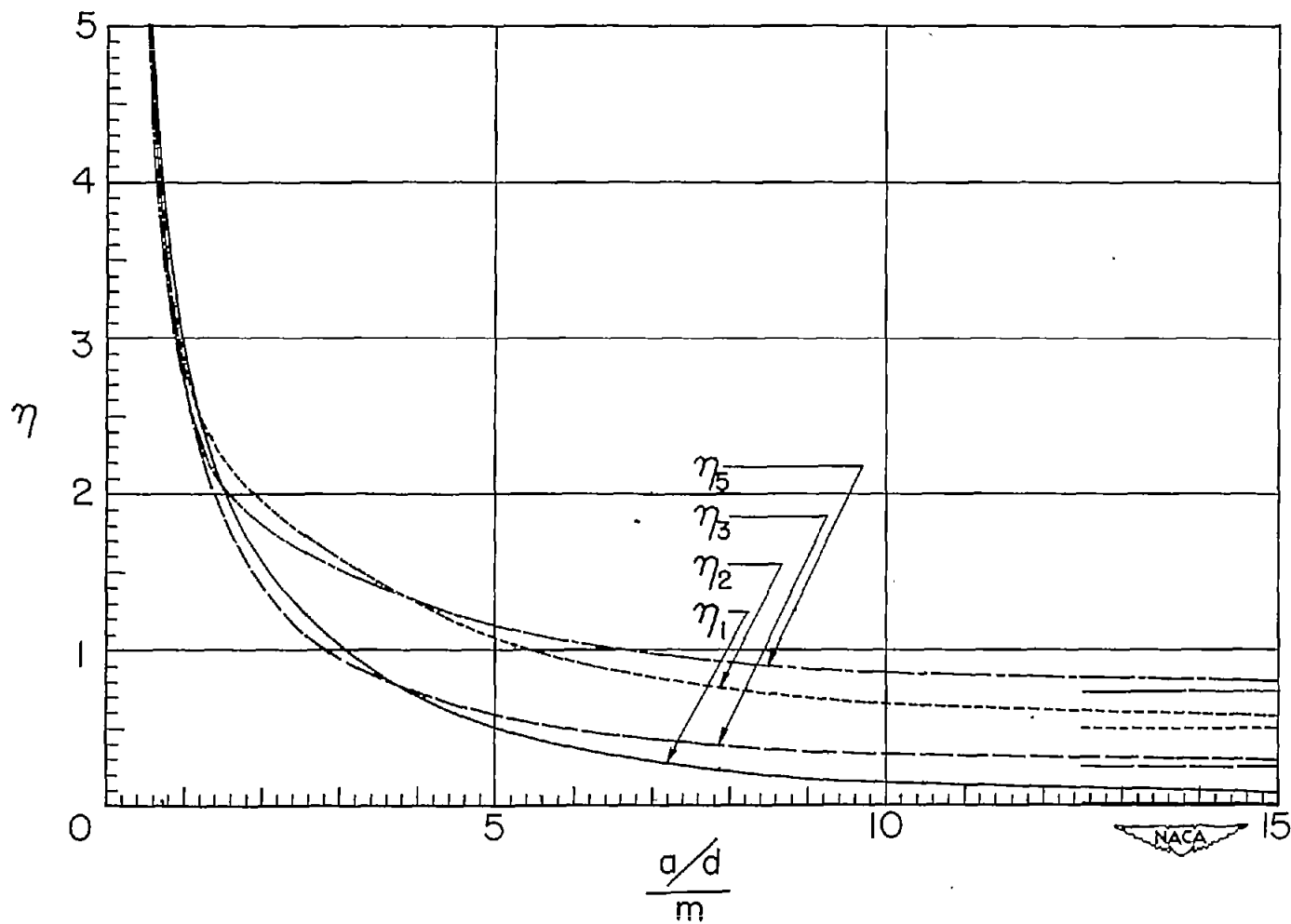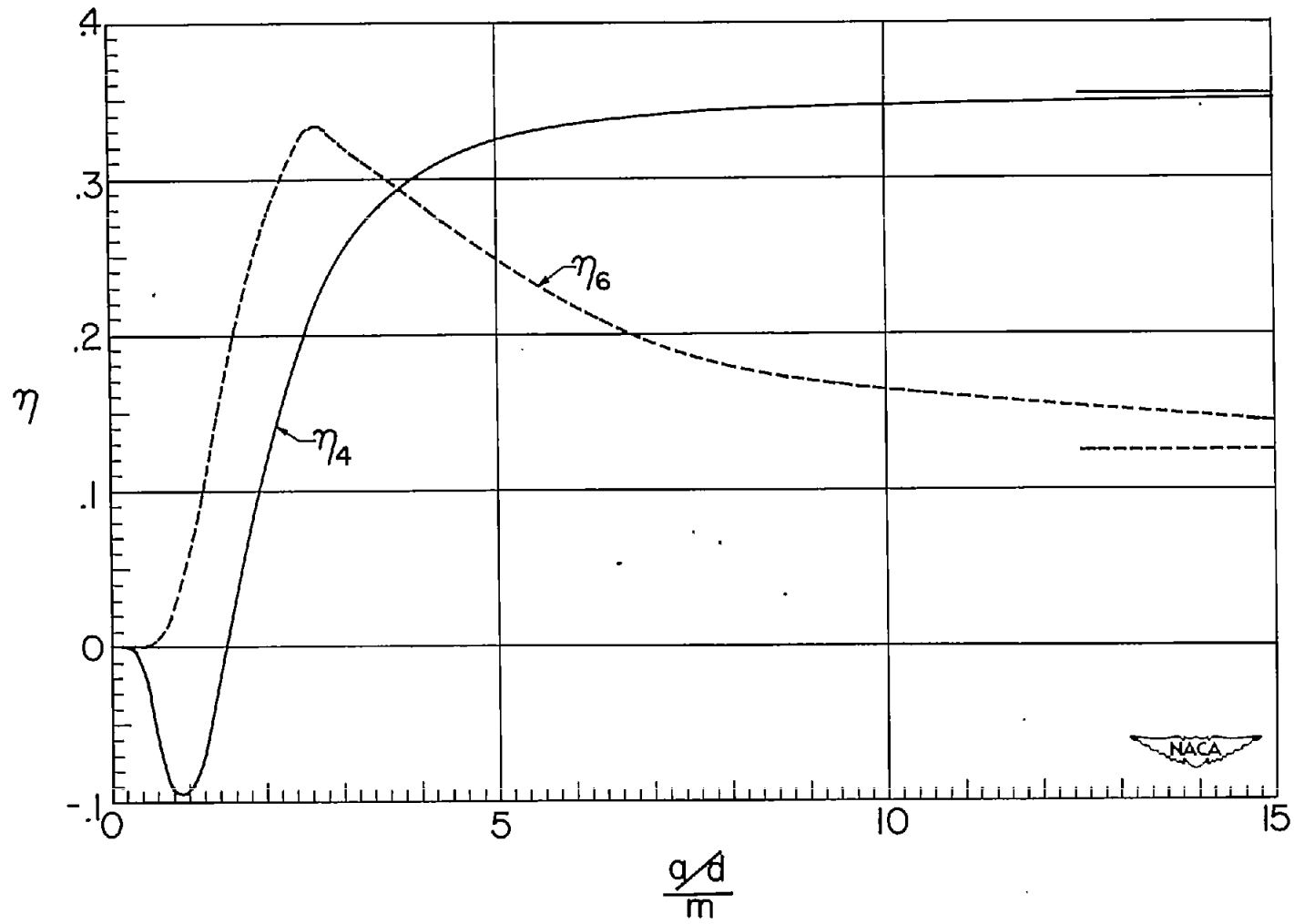Figure 2.- Hypothetical extension of stiffeners to contact line.

Figure 3.- Functions appearing in expression for effective flexural stiffness of stiffeners.
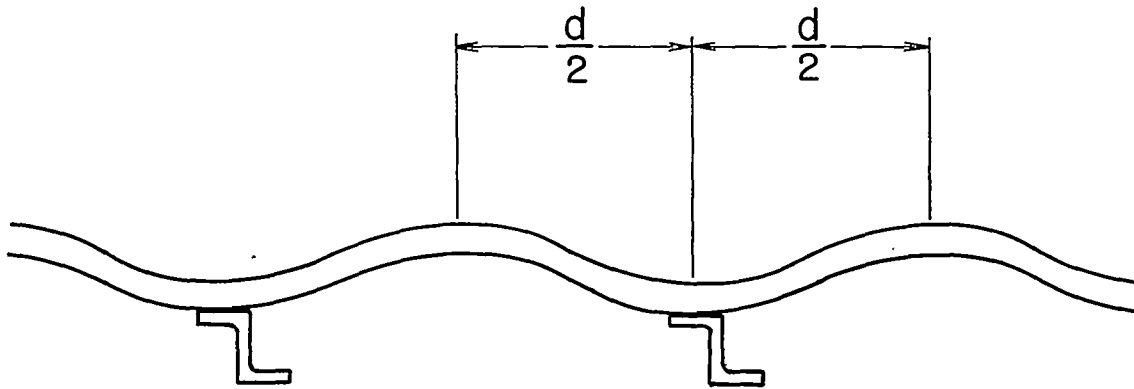
(a) η_1, η_2, η_3, and η_5.

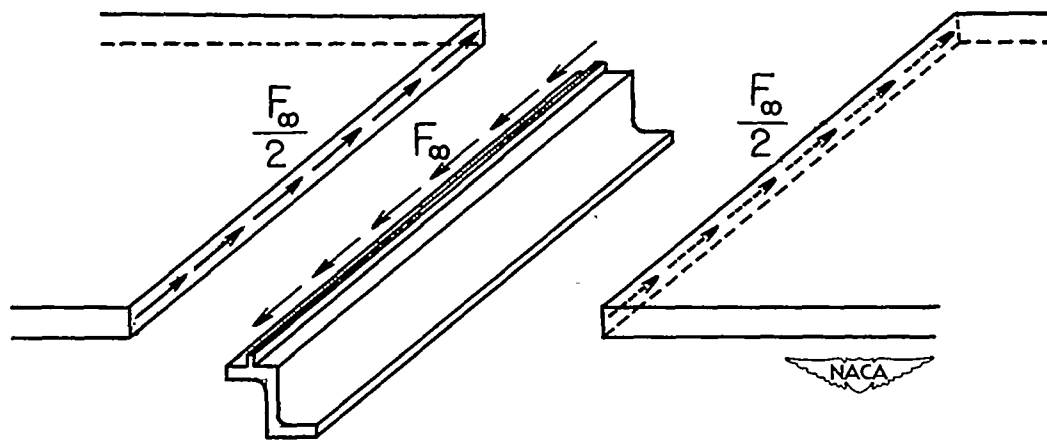Figure 4.- Functions appearing in criterion for symmetrical buckling of plate with three stiffeners.

(b) η_4 and η_6.

Figure 4.- Concluded.

(a) Shape of deflection surface in y-direction.

(b) Shear forces at contact line.

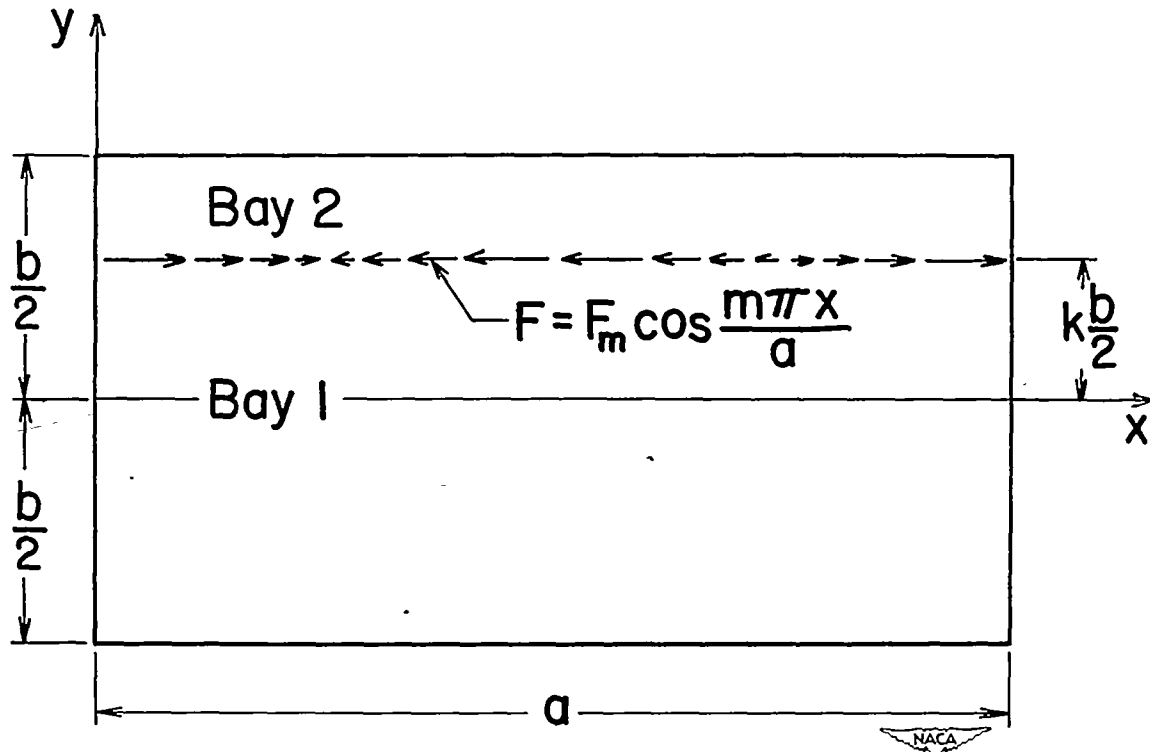Figure 5.- Conditions assumed for plate with infinitely many stiffeners.

Figure 6.- Shear force applied along a longitudinal line within the plate.